RESEARCH

A Discussion of Implausible Total Solar-Irradiance Variations Since 1700

Theodosios Chatzistergos[1] ![ORCID]

Abstract

The Sun plays a role in influencing Earth's climate, making it important to have accurate information about variations in the Sun's radiative output. Models are used to recover total solar-irradiance (TSI) variations in the past when direct space-based measurements are not available. One of the most cryptic such TSI reconstructions is the one by Hoyt and Schatten (*J. Geophys. Res*. **98**, 18, 1993, HS93). The rather vague description of the model methodology, the arbitrary selection of solar indices it employs, and the short overlap between the HS93 series and directly measured TSI values has hindered any evaluation of the performance of this model to this day. Here, we aim at rectifying this by updating the HS93 model with new input data. In this way we are also contributing in the discussion on the possible long-term changes in solar irradiance.

We find that the analysis by HS93 included a number of erroneous processing steps that led to an artificial increasing trend towards the end of the reconstructed TSI series as well as shifting the peak of the TSI in the mid-twentieth century back in time by about 11 years. Furthermore, by using direct measurements of the TSI we determined that the free parameter of the model, the magnitude of variations (here defined as percentage variations of the difference between the maximum to minimum values), is optimal when it is minimised (being ≤0.05%). This is in stark contrast to the high magnitude of variations, of 0.25%, that was imposed by HS93. However, our result is consistent with more recent estimates, such as those from the Spectral And Total Irradiance REconstruction (SATIRE) model and Naval Research Laboratory TSI (NRLTSI), which were used by the Intergovernmental Panel on Climate Change (IPCC). Overall, we find that the previously reported agreement of the HS93 TSI series to temperature on Earth was purely due to improper analysis and artefacts of the processing.

1. Introduction

The Sun is the closest star to us and enables life as we know it on Earth to exist. By providing almost all external energy to Earth's system (Kren, Pilewskie, and Coddington, 2017), the Sun is an important natural forcer of Earth's climate (Solanki, Krivova, and Haigh, 2013;

✉ T. Chatzistergos
chatzistergos@mps.mpg.de

1 Max Planck Institute for Solar System Research, Justus-von-Liebig-Weg 3, Göttingen, 37077, Germany

Krivova, 2018; IPCC, 2021). A connection between the Sun and Earth's climate was suggested centuries ago, while Herschel (1801, cf. Love, 2013) was probably the first to have explored this quantitatively. The most prominent recognised way in which the Sun affects Earth's climate is through variations in its radiative output. This is quantified as the solar radiative-energy flux as measured at the top of Earth's atmosphere and normalised to the mean Sun–Earth distance, called the solar irradiance. This is wavelength dependent, while the wavelength integral is called the total solar irradiance, TSI. Various space-based measurements of TSI have existed since 1978 (Fröhlich, 2013; Kopp, 2016). Ambiguities in the way the data could be compiled into coherent series have led to different composite series, with the most commonly used ones being ACRIM[1] (*Active Cavity Radiometer Irradiance Monitor*, which is the instrument taken as the reference by Willson, 1997 and Willson and Mordvinov, 2003), PMOD[2] (named after Physikalisch-Meteorologisches Observatorium Davos; Fröhlich, 2006), ROB[3] (named after Royal Observatory of Belgium, previously referred to as RMIB, Royal Meteorological Institute of Belgium, in French called IRMB; Dewitte, Crommelynck, and Joukoff, 2004; Dewitte and Nevens, 2016), or those by Montillet et al. (2022), and Dudok de Wit et al. (2017). The TSI composites suggest that TSI variations over the entire instrumental period were rather stable or marginally decreasing (Chatzistergos, Krivova, and Yeo, 2023).

Recovering earlier TSI values is possible only through modelling. Such models are based on the fact that TSI variations on days and longer are driven by the evolution of the solar surface magnetic field (Shapiro et al., 2017; Yeo et al., 2017). The models are divided into empirical and semi-empirical/physical ones. Empirical models use proxy indices that they scale to direct TSI measurements (e.g. Hoyt and Schatten, 1993; Lean, 2018; Chatzistergos et al., 2020a; Chatzistergos, Krivova, and Ermolli, 2024; Wang and Lean, 2021; Penza et al., 2022), in contrast to semi-empirical models that take a more physical approach (e.g. Krivova et al., 2003; Krivova, Balmaceda, and Solanki, 2007; Krivova, Vieira, and Solanki, 2010; Shapiro et al., 2011; Vieira et al., 2011; Yeo et al., 2014; Dasi-Espuig et al., 2016; Egorova et al., 2018; Wu et al., 2018; Chatzistergos et al., 2021; Ermolli and Chatzistergos, 2023).

There have been quite a few TSI reconstructions covering the last four centuries, using either sunspot-number series or cosmogenic radioisotopes (for a review see Chatzistergos, Krivova, and Yeo, 2023). The various TSI reconstructions show disagreement by about an order of magnitude on the secular trend of variations (Chatzistergos, Krivova, and Yeo, 2023). However, due to improvements in data recovery and calibrations, as well as improved understanding of solar variability, there have been several studies constraining the magnitude of possible TSI variations (e.g. Lockwood and Ball, 2020; Yeo et al., 2020; Marchenko, Lean, and DeLand, 2022). A conservative, but robust, such constraint was given by Yeo et al. (2020) who determined that the dimmest state the Sun could be is 2 ± 0.7 W m^{-2} lower than the value over 2019. Despite the general agreement for lower estimates of the secular trend in TSI, the uncertainty in its actual value still abides. Furthermore, we note that the estimates of the global temperature sensitivity to solar forcing currently range roughly between 0.07 and 0.10 K (W m^{-2})$^{-1}$ (e.g. Misios et al., 2016; Amdur, Stine, and Huybers, 2021), which, however, depends on the solar forcing dataset used and thus carries the uncertainty associated with it.

Notwithstanding all the advances briefly summarised here, several old and outdated TSI reconstructed series are still frequently used in the literature. For example, Connolly et al.

---

[1] Available at https://web.archive.org/web/20170611210135/http://acrim.com/.

[2] Available at https://www.pmodwrc.ch.

[3] Available at https://www.sidc.be/observations/space-based-timelines/tsi.

(2021, 2023) and Soon et al. (2023) have asserted that "most (if not all) of the Northern Hemisphere warming trend since the 19th century (and earlier) has been due to solar variability" by mostly focusing on two such outdated TSI reconstructions by Bard et al. (2000) and Hoyt and Schatten (1993, HS93, hereafter). Connolly et al. (2021) even stated that "the Hoyt and Schatten (1993) estimate suggests that 98% of the long-term trend (1841 – 2018) of the rural-only temperature estimates can be explained in terms of solar variability". The Bard et al. (2000) and HS93 reconstructions used concentrations of cosmogenic radioisotopes and various sunspot indices, respectively. It is important to stress that the magnitude of TSI variations on both of those TSI series was imposed based on assumptions from Sun-like stars that eventually were shown to be incorrect (e.g. Hall and Lockwood, 2004; Hall et al., 2009; Wright, 2004). The series by Bard et al. (2000) was eventually updated by Delaygue and Bard (2011), while more advanced reconstructions with cosmogenic radioisotopes followed too (e.g. Vieira et al., 2011; Wu et al., 2018), which suggested a significantly lower secular trend than the original series by Bard et al. (2000).

The HS93 series is one of the most cryptic TSI reconstructions. It is a purely empirical TSI reconstruction model, which uses as input a combination of five indices of solar activity, namely the sunspot-number series, solar-cycle lengths, solar-cycle-decay rate, equatorial rotation, and fraction of "penumbral" sunspots. The choice of these indices was argued by HS93 by providing rather approximate empirical relations to individual sunspot-decay rates, instead of directly comparing the indices and final reconstruction to directly measured TSI. The vagueness in the description of the HS93 model has contributed in hindering any replication and update of this model with newer data so far. The HS93 TSI series has only been extended by simply stitching it to the ACRIM TSI composite followed by SORCE/TIM (*Total Irradiance Monitor* onboard the *Solar Radiation and Climate Experiment* mission; Kopp, 2021) and TSIS-1/TIM (*Total and Spectral Solar Irradiance Sensor*; Pilewski et al., 2018) data (as done, e.g., by Scafetta, 2013, 2023; Scafetta et al., 2019). However, this process provides no new insights on the performance of the model or its aptness to recover past irradiance variations. On the contrary, this has the potential of introducing artificial trends in TSI and lead to unrealistic estimates of past irradiance variations.

In this work, we aim at contributing to the discussion of possible secular variations of TSI. In particular, we replicate and discuss the modelling approach by HS93 to assess its performance and aptness for reconstructing past irradiance variations. In this way we can also assess the merit of recent claims of high solar impact on recent Earth's climate change based on the HS93 model. We use modern data to extend the various sunspot indices used by HS93 and thus allow for a direct comparison to TSI measurements. We introduce the solar-activity indices used by HS93 in Section 2, as well as update them with more recent data and discuss issues with their derivation. We present our results on reconstructing TSI with the HS93 model in Section 3. We compare the reconstructed TSI with the HS93 model to Earth's temperature in Section 4 and draw our conclusions in Section 5.

2. Breaking down the HS93 Model

In this section we introduce and discuss separately each of the solar-activity indices used in the HS93 model. In particular, we first extract the indices as used by HS93 from their Figure 8, unless otherwise stated, and then we update each index by replicating HS93's methodology with current data. The indices in Figure 8 of HS93 have already been converted to TSI values, thus in this section we linearly scale them to our results to allow a

Table 1 Indices used in the HS93 model. Uncertain entries for the case of HS93 are denoted with *.

Index	Data used by HS93		Data used in this study		Cadence	Smoothing
	Source	Period	Source	Period		
Sunspot number	ISNv1	1700 – 1992	ISNv2	1700 – 2023	Annual	11-year
Cycle length	ISNv1	1700 – 1992	ISNv2	1700 – 2023	Annual	23-year
Cycle-decay rate	ISNv1	1739 – 1972*	ISNv2	1749 – 2023	Monthly*	5-year*
Equatorial rotation	RGO	1874 – 1976	RGO	1874 – 2016	Daily	Cycle mean
Penumbral spots	RGO, Rome	1874 – 1989	RGO, Rome and Debrecen	1874 – 2018	Daily	11-year

direct comparison. However, we note that the low quality figures in the HS93 paper sometimes make it difficult to disentangle the indices accurately enough. We also note here the difficulty in identifying exactly the methodology used by HS93 to produce the indices. This is particularly aggravated due to HS93's discussion focusing mostly on relating the indices to individual sunspot-decay rates, rather than providing a complete and clear description of their methodology. For this reason, we have also consulted Hoyt and Schatten (1997) where the same authors describe the HS93 model too. Personal communication with the authors did not provide any additional clarifications that could help to resolve the ambiguities with the methodology. The main characteristics of each index are summarised in Table 1.

2.1. Sunspot-Number Series

The first solar-activity index used by HS93 is the sunspot-number series (Clette and Lefèvre, 2016, ISN) shown in Figure 1. For this index HS93 appear to have used version 1 of ISN (ISNv1), which was the main sunspot-number series available at the time that extended back to 1700 with annual values (monthly values extend back to 1749, while daily values exist only since 1818). Possible alternative series such as the Boulder sunspot number, the American Association of Variable Star Observers (AAVSO) sunspot number, or the Royal Observatory, Greenwich (RGO) database (see Hathaway, 2015, for an overview), are excluded since they do not cover the entire period of the HS93 reconstructions, i.e. 1700 – 1992.

HS93 considers this index twice, once as annual means and also as 11-year running means. HS93 further shifted the 11-year smoothed sunspot number by 11 years to the past. HS93 base this on an argument by Dicke (1979) that asserts that there is a 13-year delay between changes in solar luminosity and the manifestation of magnetic field on the solar surface. The work by Dicke (1979, cf. Weisshaar, Cameron, and Schüssler 2023, Biswas et al. 2023) was published shortly after the first space-based measurements of TSI and thus such speculations could not be evaluated at that time. However, subsequent studies have revealed that irradiance variations are indeed driven by solar-surface magnetism (Shapiro et al., 2017; Yeo et al., 2017). Based on this, models have succeeded at replicating irradiance variations from observations of solar surface magnetic field with exceptional accuracy without any need for such a 11- or 13-year delay between sunspots and irradiance changes (e.g. Shapiro et al., 2017; Yeo et al., 2017; Chatzistergos, Krivova, and Yeo, 2023). This is rendering the claim for the need of a 13-year offset between solar surface magnetism and solar-irradiance variations to be unfounded. Furthermore, HS93 do not provide any justification why instead of 13 years given by Dicke (1979) they used 11 years or why they arbitrarily used this offset for only some of the sunspot indices. For instance, this lag was introduced on the 11-year smoothed sunspot-number series, but it seems it was not applied on the annual cadence sunspot-number series.
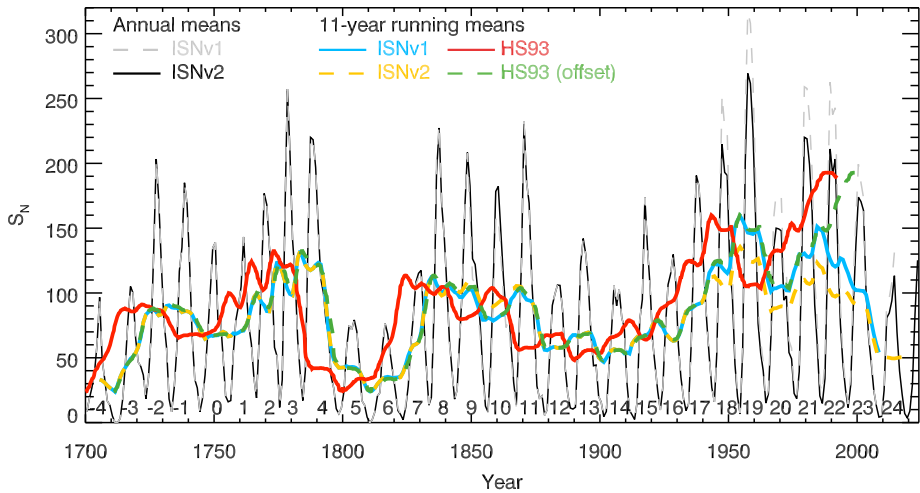
Figure 1 Sunspot-number series. Shown are annual values of ISNv1 (dashed grey) and ISNv2 (black) as well as 11-year running means of ISNv1 (ciel), ISNv2 (dashed yellow), and the sunspot-number series used by HS93 digitised from their Figure 8 and scaled to ISNv1 (red). Since the sunspot-number series used by HS93 was offset by 11 years to the past, we also show it by restoring it to the original time period (dashed green). The numbers at the lower part of the figure denote the conventional solar-cycle numbering.

In order to have this index cover until the end of 1992 after shifting it by 11 years in the past, HS93 had to extend the sunspot-number series to the end of 2003, 11 years after the time of writing of their paper. This is not mentioned in HS93 or Hoyt and Schatten (1997), while Figure 1 suggests that they predicted a steady and linear increase in sunspot number for the decade that followed their publication. This prediction of HS93 for the sunspot number did not materialise, evidenced by a decrease in the 11-year smoothed ISNv1 over the years that followed the publication of HS93 which can be seen in Figure 1. It is noteworthy that among all indices used by HS93, the smoothed sunspot-number series was the one exhibiting the sharpest increase since 1960s. Thus, the biggest contribution for the increasing trend since the 1960s in the HS93 series was indeed an artefact.

Since the publication of HS93 there has been an extensive effort to correct mistakes in the existing sunspot databases (e.g. Arlt et al., 2013; Vaquero et al., 2016; Hayakawa et al., 2021b), recover more raw data (e.g. Hayakawa et al., 2021a; Carrasco, Vaquero, and Gallego, 2021; Carrasco et al., 2021; Ermolli et al., 2023), as well as improve the cross-calibration techniques used to compile the available data (e.g. Usoskin et al., 2016; Usoskin, Kovaltsov, and Chatzistergos, 2016; Chatzistergos et al., 2017; Bhattacharya et al., 2023; for a review see Clette et al., 2023). In 2016, a new version of ISN was released (ISNv2), which applied corrections to the composite series for some identified inconsistencies (Clette and Lefèvre, 2016). ISNv2 also changed the reference observer and thus the level of ISN too. However, since this is a fixed scaling factor, in our discussion we will present results in the scale of ISNv2 and always scale by 1.67 all earlier versions to bring them to the scale of ISNv2. A key correction that is important for our discussion is the so-called "Waldmeier" jump. That is an artificial inflation of sunspot numbers since the late 1940s (Waldmeier, 1961; Clette et al., 2021). Thus, accounting for this issue, reduces the overall level of sunspot numbers after 1940s relative to earlier periods. Since HS93 relied on ISNv1 it also suffered from these now-corrected artefacts that are associated with ISNv1.

For our replication of this index we use ISNv2, once as annual means and once with an 11-year smoothing (shown in Figure 1). However, we do not consider the 11-year temporal lag introduced by HS93.

2.2. Solar-Cycle Length

The second index used by HS93 is the length of the solar cycle. This series also covers the period 1700–1992 and thus was produced from the annual ISNv1 series (see Section 2.1).

We note that this cycle-length series is not mentioned by Hoyt and Schatten (1997) at all, while the description HS93 give about their process to obtain the cycle lengths is the following: "Each year has a level of activity which may be expressed as a percent of the maximum level of activity for the cycle it belongs to. For each year one may find the cycle lengths by measuring the elapsed time between equal percentage levels of activity. Two cycle length determinations are made each year in this approach, so nearly all the data are used rather than selected extremum points in the cycle. A 23-year running mean was then applied to obtain the final results."

This description is unfortunately rather vague and unclear. Below, we describe two different interpretations we used in our attempt to replicate the HS93 cycle-length series:

- For the first interpretation we produce the cumulative sum of values within each cycle and then normalise them to unity. In this way the series has the value of 0 at the beginning of the cycle and the value of 1 at the end. We then compute for each year the time difference between the same value in the next and previous cycle.
- For the second interpretation we start by applying a 4-year running mean to the sunspot numbers and then divide them with the maximum value within each cycle. In this way the series obtains the value of 1 at solar maximum and the value of 0 at minimum. We then compute for each year the time difference between similar levels of activity within the time intervals of [-7, -15] and [7, 15] years.

The cycle length for each year is the average of the two computations. For the years for which there is no previous/next cycle we keep only one value, however, we stress that this is less accurate than for the rest of the values. Finally, we apply a 23-year running mean. Due to this smoothing the last 12 years should be excluded in order to treat the data consistently. The cycle-length series presented by HS93 extended up to the end of 1992, which means that the values over the last cycle have different statistics and can lead to artefacts. For both interpretations we need an initial guess of the start of solar cycles, for which we use the values defined by SILSO[4] (Sunspot Index and Long-term Solar Observations). The final cycle-length index used by HS93 is considered with a reversed ordinate, which means that for the following discussion a decrease in cycle length means an increase of the cycle-length index and it is associated with an increase in TSI.

Figure 2 compares our cycle-length series to the one by HS93 and Chatzistergos (2023, computed as the time difference between cycle extrema and then smoothed). We find both of our interpretations show qualitatively the same behaviour as those by HS93 and Chatzistergos (2023), however, with some noticeable differences. For instance, the first interpretation results in a significantly smoother curve than with the second interpretation or the one by HS93. Although we consider the overall definition of our first interpretation of the cycle-length series to be more reasonable than the second one, the second one shows a better match with the one by HS93. Furthermore, both interpretations rely on the estimates of the

---

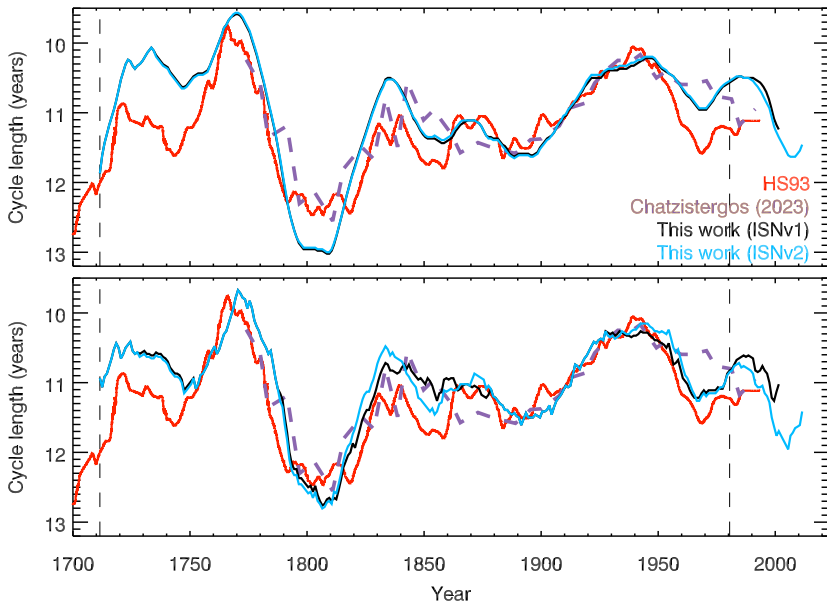[4]https://www.sidc.be/SILSO/cyclesminmax.

Figure 2 Cycle-length series replicating the methodology of HS93. We show separately the result for interpretations 1 and 2 at the top and bottom panels, respectively (see Section 2.2). Also shown are the cycle-length series by HS93 (red) and the one by Chatzistergos (2023, dashed purple). The vertical dashed lines mark the years beyond which the HS93 series is not meaningful due to the smoothing process.

cycle extrema, which might be a source of discrepancy between our results and those by HS93. However, HS93 do not provide any information on this and we do not know how they determined the cycle-extrema dates. Overall, as Figure 2 demonstrates, the results are effectively unaffected by the version of ISN that is used. In the following, we will use the cycle-length series we produced with the second interpretation using ISNv2.

Furthermore, we remind the reader of the Waldmeier rules (Hathaway, 2015; Usoskin, Kovaltsov, and Kiviaho, 2021; Similä and Usoskin, 2022; Chatzistergos, 2023) that connect the length of a solar cycle with the amplitude of the next cycle. Thus, HS93 by offsetting the sunspot-number series by 11 years to the past they improved the agreement between the cycle-length series and the smoothed sunspot-number series, but they also erroneously displaced the peak of these indices by 11 years to the past (see also, e.g., Pesnell, 2016; Nandy, 2021; Petrovay, 2020).

2.3. Solar-Cycle-Decay Rate

The third index used by HS93 is the rate of solar-cycle decay. This is the most vague index used by HS93 without a direct description on how it was produced. We also note that Soon, Connolly, and Connolly (2015) erroneously mention that this index is the annually resolved cycle-length series we introduced in Section 2.2. In HS93 we find the following relevant segments: "Solar-cycle lengths can be split into a rise time from sunspot minimum to sunspot maximum and a decay or fall off time from the maximum to the next minimum. [...] From the above discussion we expect a more rapid decay of the activity cycle to be associated with more rapid decay of individual sunspots and with shorter solar-cycle lengths. Hence, the change in downward slope can be used as another proxy to monitor long-term secular

changes in the Sun. Dividing the mean cycle-decay rate of the Wolf sunspot numbers by the maximum Wolf number of the cycle gives a normalized cycle-decay rate. This normalization simply removes the variations arising from variations in the rate of sunspot generation." They follow this with a linear relationship between the cycle-decay rate and the sunspot-decay rates and the following text: "$R_{z,\max}$ is the smoothed sunspot maximum published by Waldmeier [1961] used to normalise the sunspot-decay rate to a decay rate per group and $|(dR_z/Dt)_{\max}|$ is the absolute value of the mean cycle-decay rate per year averaged over 5 years." From these sentences arises the ambiguity of whether HS93 used the cycle decay or the normalised cycle-decay rate to reconstruct the TSI. We will test both cases in the following.

The cycle-decay rate used by HS93 can be seen in Figure 3. We note that this index extends between 1739 and 1972, however, due to the series being very faint in HS93's Figure 8 and its end being rather close to other series, it might be that the series extends further than 1972, which we could not discern, potentially partially overlapping with another index. The beginning of the series is more readily seen and it is better defined at 1739. We consider two possibilities, either HS93 ignored the first 39 years of the annual ISNv1 when constructing this index, or they used the monthly ISNv1, which starts in 1749, and offset it by 10 years in the past. We could not find a justification as to why HS93 would ignore the first 39 years of this index in the case they had used the annual sunspot-number series, thus we consider the second option more likely, even though HS93 do not explicitly mention such an offset for this index. A personal communication with Douglas Hoyt did not allow us to resolve the ambiguities with the construction of this index, however, it suggested that our above interpretation of having offset this index by about 10 years to the past is probably correct.

Based on the above, we produce the solar-cycle-decay rate as:

$$d_i = \frac{R_{z,i}^{\max} - R_{z,i}^{\min}}{T_{R_{z,i}^{\max}} - T_{R_{z,i}^{\min}}}, \tag{1}$$

where d_i is the cycle-decay rate of the ith cycle, $R_{z,i}^{\max}$ and $R_{z,i}^{\min}$ the maximum and minimum sunspot number within each cycle, and $T_{R_{z,i}^{\max}}$ and $T_{R_{z,i}^{\min}}$ the time of cycle maximum and minimum. We then produce the normalised cycle-decay rate by dividing the cycle-decay rate by the maximum sunspot number within each cycle. We use the monthly values of ISNv2 to produce the above series. The series we digitised from Figure 8 of HS93 suggests heavy smoothing and not just using a cycle-averaged value, as would be expected for the cycle-decay rate. Therefore, to try to reproduce this we first apply a linear interpolation so that the series has annual values and not just one for each solar cycle, and then apply a 5-year running smoothing.

For comparison purposes and since it was mentioned by HS93 we also use the data presented by Waldmeier (1961). These include the cycle-decay period, rise period, highest and smallest smoothed monthly sunspot number, as well as the years of cycle minimum and maximum, extending back to 1750 (although information on rise/decay periods goes back to 1610). Based on the information in Waldmeier (1961) we can readily produce the cycle decay and normalised cycle-decay rates as defined above.

Figure 3 compares our results to the cycle-decay series we digitised from HS93 and those we produce with the data by Waldmeier (1961). Comparing the normalised decay rates we note that the series agree on the main peak being at about 1830, while the one from Waldmeier (1961) data also replicates a smaller peak found in the HS93 series in the 1890s. However, overall we find noticeable differences between the various normalised cycle-decay rates, with the striking difference that the series do not cover the same periods.
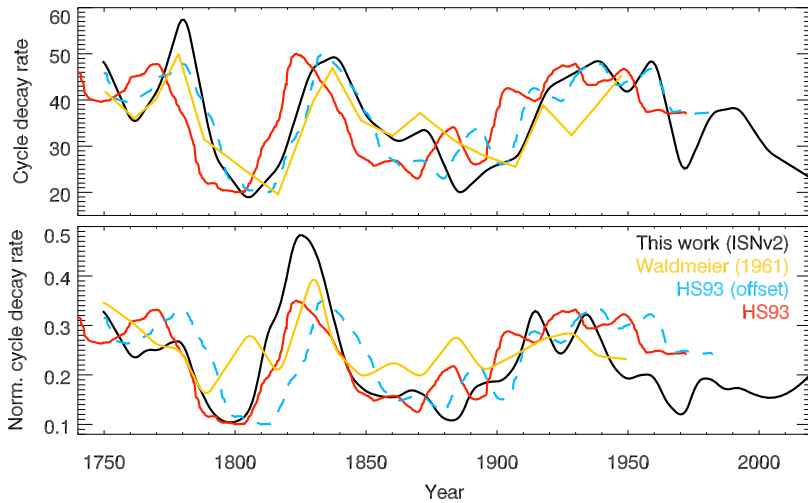
Figure 3 Solar cycle-decay rates (sunspot number per year; top panel) and normalised cycle-decay rates (bottom panel) following HS93. Our produced series is shown in black, while the series we digitised from HS93 is shown in red after scaling it to roughly match our series. We also show a series produced from the data by Waldmeier (1961, yellow) as well as the HS93 series by offsetting it by 10 years (dashed ciel).

A better agreement is found between the HS93 cycle-decay rate and our series without the normalisation, albeit when applying an offset of about 10 years. In this way we replicate the cycle-decay rate by HS93 rather well, except over the period 1860 – 1900 when we notice the largest differences. However, over that period there are differences from the series produced with the data by Waldmeier (1961) too.

Based on the above, we consider that HS93 used the monthly ISNv1 series to produce the cycle-decay rates, which they then offset by 10 years in the past. We consider that the discussions for normalised decay rates were simply their attempt to connect the cycle-decay rates to individual spot decay rates, while the cycle-decay rate (that is without the normalisation) must have been used for the irradiance reconstruction. Therefore, in the following we will use the cycle-decay rate, without the normalisation, we computed from monthly ISNv2 series.

2.4. Equatorial Solar Rotation

The fourth index used by HS93 is the equatorial solar rotation. HS93 took this index from Hoyt (1990) where the derivation process is also described. This index extends between 1874 and 1976, because it relies on the RGO[5] database. Since the publication of HS93 the RGO and U.S. Air Force (USAF) National Oceanic and Atmospheric Administration (NOAA)[5] database has incorporated more data, now extending until 2016. This database includes information about area, latitude and longitude on the solar disc for individual sunspot groups. The database has also given an id number to each region, which allows us to match the same regions in records for different days. We repeated the process to derive the equatorial solar rotation from the RGO/USAF/NOAA database. We note that there are various studies of equatorial rotation from sunspot data (e.g. Sakurai, 1977; Javaraiah, Bertello, and

---

[5]Available at https://solarscience.msfc.nasa.gov/greenwch.shtml.

Ulrich, 2005; Javaraiah, 2011; Jha et al., 2021; Mishra et al., 2024), applying different approaches. However, since our aim here is to replicate the index used by HS93 we follow the methodology by Hoyt (1990).

In particular, the process is as follows. We first excluded all sunspot groups with an absolute distance to the central meridian that is greater than 60 degrees or that their absolute latitude is greater than 5 degrees. Then, for each group we computed its synodic rotation by computing the change in meridional distance to its previous appearance divided by the elapsed time. Then, we converted the synodic rotation period to sidereal with the following formula (Roša et al., 1995; Wittmann, 1996; Skokić et al., 2014):

$$\Omega_{\text{sidereal}} = \Omega_{\text{synodic}} + \frac{\overline{\Omega}_{\text{Earth}}}{r^2}\left(\frac{\cos^2\psi}{\cos i}\right), \tag{2}$$

where $\overline{\Omega}_{\text{Earth}}$ is the mean orbital angular velocity of the Earth (0.9856°/day), i is the inclination of the solar equator to the ecliptic, ψ is the angle between the pole of the ecliptic and the solar rotation axis orthographically projected on the solar disk, and r is the Sun–Earth distance in astronomical units (Lamb, 2017; Jha et al., 2021).

Figure 4a shows the distribution of Ω_{sidereal} for all sunspot groups in the RGO/USAF/NOAA database, as well as for only those before 1976 that was the period used by HS93. We note that the database is plagued with many instances that the resulting value of equatorial rotation is not realistic. We find extreme values of equatorial rotations of 0.8°/day up to 73°/day (or 5.5°/day up to 72.5°/day when considering only the data up to 1976 that was used by HS93). We note that the database has undergone various corrections (that can affect the date/time of observations as well as the latitude/longitude or id group number) over the years and it is likely that the version HS93 used had more problematic cases than the ones included in the current version of the database. For our analysis we consider values below 11°/day and greater than 18°/day to be artefacts due to mistakes in the database, so we exclude them. Figure 4b shows the daily mean values for the differential rotation. Several periods are seen with clumps of erroneous rotation values, e.g. around 1910, 1940, and 1970. Furthermore, after the end of RGO in 1976 the values of meridional distances are listed as integer values, and thus are less precise than the earlier data, which introduces a discontinuity in the differential rotations derived from these data. In Figure 4b we also show in ciel the equatorial rotation after 11-year smoothing showing that it is rather stable, with only minor changes.

We then compute the rotation period as:

$$P = 360°/\Omega_{\text{sidereal}}. \tag{3}$$

This is the equatorial rotation index that was used by HS93 to reconstruct the TSI.

Figure 4c compares our produced rotation-period series to that by HS93. In particular, we digitised this index from Table 2 of Hoyt (1990) and Figure 8 of HS93, both shown in Figure 4c in yellow and red, respectively. From HS93 Figure 8 we can see that instead of using the cycle-averaged series, they seem to have assigned the cycle-averaged value to the central year of the cycle and then linearly interpolated for the remaining years. Some smoothing might have been applied too, but it is very difficult to understand this due to the poor quality of their Figure 8. As an indication of them having applied some smoothing is the shape of the curve over 1970s that has the same behaviour of leveling and then slightly decreasing as seen in all other indices in their Figure 8 where they applied some smoothing.

We note the rotation period exhibits rather small changes, however, it is unclear if they are meaningful or if they are due to issues in the databases. We note also that HS93 recognised
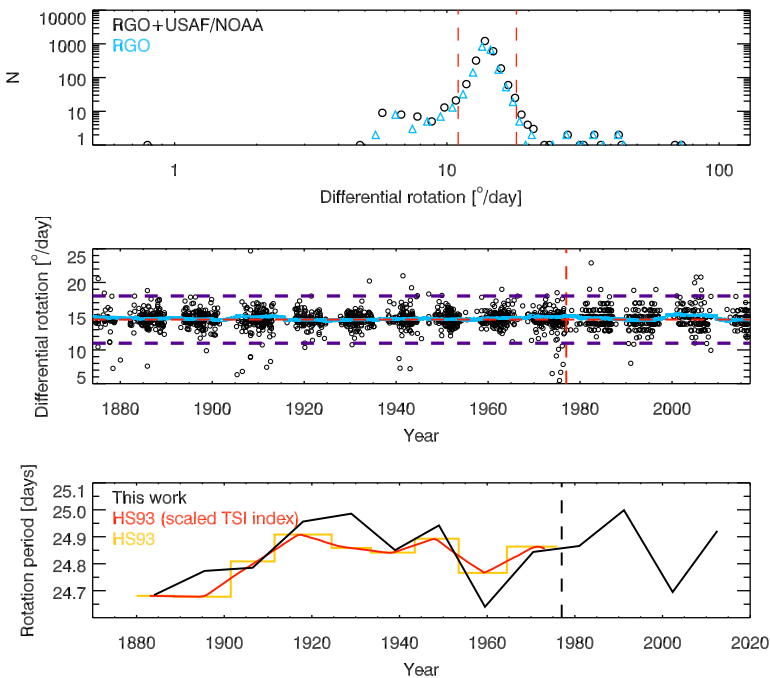
Figure 4 *Top:* Distribution of equatorial rotation values produced from the RGO and USAF/NOAA data (black). We show separately only the RGO data before 1977 in ciel. The vertical dashed red lines mark the thresholds we used to exclude potentially problematic values. *Middle:* Evolution of determined daily values of equatorial rotation from RGO and USAF/NOAA data (black for daily values, and ciel for 11-year running means). The vertical red dashed line marks the switch between the RGO and USAF/NOAA data, while the horizontal dashed purple lines denote the thresholds we used to exclude potentially problematic values, and the horizontal red line denotes the mean value of differential rotation (14.5°/day). *Bottom:* Equatorial rotation period index as defined by HS93 (see Section 2.4) and produced here with the RGO/USAF/NOAA sunspot data (black). We also show the index digitised from Table 2 by Hoyt (1990, which is the same as shown in HS93 Figure 1; yellow) and HS93 Figure 8 (red; this was the form of the index they used for producing the TSI series). The vertical dashed line denotes the switch between the RGO and USAF/NOAA data, which introduced a discontinuity in the data.

that such changes in equatorial rotation might not be meaningful considering that they stated: "The solar rotation model has two peaks which arises, in part, from the difficulty of obtaining a good measure of solar rotation with the few observations available." Our series exhibits two peaks too, however, the first peak in our series happens for one cycle after the one in the HS93 series. There is a marked discontinuity in our series after 1976 when the RGO data ended, however, the change is again rather small.

Furthermore, we stress that issues with early RGO group counts have been mentioned (Sarychev and Roshchina, 2009; Clette et al., 2014; Cliver and Ling, 2016; Lockwood et al., 2016) which might affect the records potentially up to 1900 or even 1915. Thus, the equatorial rotation index determined from RGO data is uncertain over the period before 1915, thus also the sharp increase that this index exhibits over that period might be an artefact due to residual issues with the data.

Having stressed potential issues with the variations in this index, in the following we will use the series we produce with RGO/USAF/NOAA sunspot data as shown in Figure 4c in black.
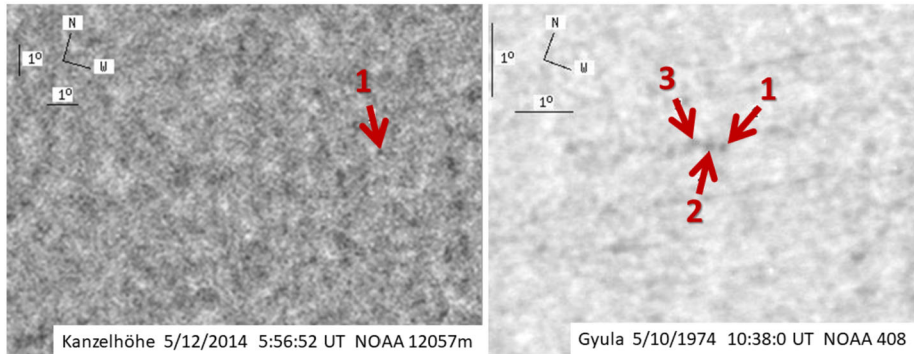
Figure 5 Examples of "penumbral spots" in the Debrecen database. Shown are groups from the Kanzel-höhe observation made on 12 May 2014 (left: http://fenyi.solarobs.epss.hun-ren.hu/DPD/2014/20140512/20140512_12057m.html) and Guyla observation made on 10 May 1974 (right: http://fenyi.solarobs.epss.hun-ren.hu/DPD/1974/19740510/19740510_408.html). All identified spots within these "penumbral spot" groups are numbered and marked with red arrows.

2.5. Fraction of Penumbral Sunspots

The last index used by HS93 is the fraction of penumbral spots. This is a rather peculiar index to be considered for irradiance reconstructions, particularly since, to the best of our knowledge, there is no formal definition of "penumbral sunspots". What is termed "penum-bral sunspots" by HS93 are sunspot groups, not individual spots, that are listed in databases as the entire group having no umbral area, but a total sunspot-group area greater than 0 (typically meaning greater than or equal to 1 msd). They are found in at least the databases of RGO,[5] Rome,[6] and Debrecen[7] (Baranyi, 2015). Two exemplary images from the Debrecen catalogue with identified sunspot groups that are considered "penumbral spots" are shown in Figure 5. These appear to be small features with intensities rather similar to that of the quiet Sun. Such regions are highly uncertain considering the difficulty in identifying which regions are indeed spots if umbra is not resolved or is too faint. Furthermore, it is likely that at least some of these regions are simply artefacts that have been mislabeled as spots.

Further aggravating this is that it is unclear how the umbra/penumbra separation was done in all archives. In RGO and Rome the identification was done manually, which then carries the extra uncertainty of potential variations of the selection criteria over time. In Debrecen this was most likely done in an automatic way with fixed intensity thresholds. Therefore, the observing conditions can significantly affect the measurements, e.g. when there is poor seeing the spots would appear smeared and the umbra will appear brighter and potentially indistinguishable from the penumbra. Overall, it is highly uncertain whether this index can be used for studying solar variability. We also note that there have been mentions of how inclusion of these "penumbral" features distorts the sunspot-number series (Lefevre and Clette, 2014). Therefore, it comes as a surprise reading HS93 stating that: "The fraction of penumbral spots model has more year to year variability than the other models and is probably picking up real solar variations which the other models cannot resolve."

HS93 produced the penumbral-spot index by simply obtaining the fraction of sunspot groups within a year that had only penumbra to all sunspot groups. They used the data from

---

[6]Available at https://www.ngdc.noaa.gov/stp/solar/sunspotregionsdata.html.

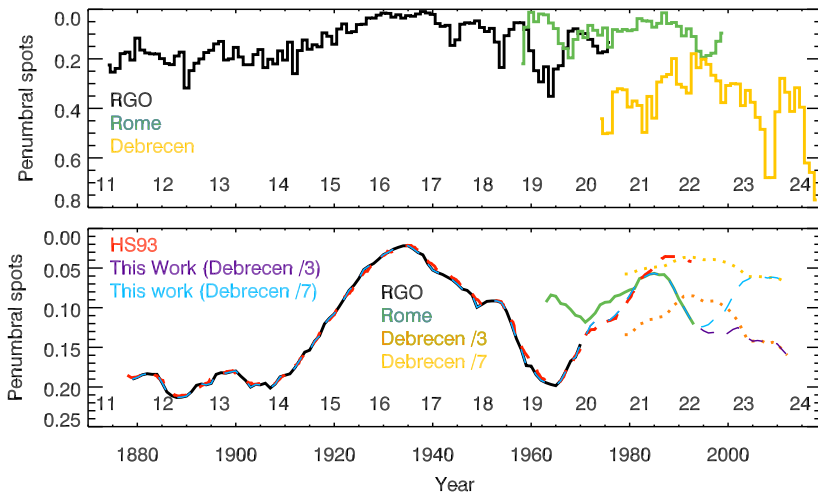[7]Available at http://fenyi.solarobs.epss.hun-ren.hu/en/databases/DPD/.

Figure 6 Fraction of penumbral spots. The top panel shows annual values, while the lower panel shows the indices after 11-year running smoothing. The data shown are from the RGO (black), Rome (green), and Debrecen (yellow) databases. Also shown in the lower panel are the penumbral-spot index by Hoyt and Schatten (1993, dashed red), scaled penumbral-spot fractions from Debrecen (divided by 3 in dotted orange and by 7 in dotted yellow) and a series by combining the RGO data with Rome ones after 1976 and the scaled Debrecen ones after 2000 (dashed ciel for Debrecen divided by 7 and dashed purple for Debrecen divided by 3). To improve the visibility of the curves in the lower panel we show them in a reduced range compared to the top panel, which, however, does not allow us to show the original unscaled Debrecen data. The numbers at the lower part of the figures denote the conventional solar-cycle numbering.

RGO, which they extended until the end of 1989 with data from Rome observatory and applied an 11-year running smoothing.

Figure 6a shows the fraction of penumbral spots from RGO, Rome, and Debrecen databases separately without any smoothing. It becomes very clear that the overall behaviour of penumbral spots is significantly different in the various databases. Rome and RGO report between 20 – 40% of spots having only penumbra, while this increases significantly for Debrecen to about 20 – 80%. The evolution of penumbral spots differs dramatically between the different archives, showing opposite behaviours over almost the entire overlapping periods. Peculiarly, around 1995 there is an increase in penumbral spots in the Rome database, at the same time of a decrease of penumbral spots in the Debrecen database. Similarly, between 1955 and 1965, when Rome shows a decrease in penumbral spots, RGO reports an increase. Overall, the level of penumbral spots is relatively stable in the Rome database, while the RGO one shows a consistent decrease until the 1940s, which is followed by an increase. Debrecen data show an increase since the 1990s.

Figure 6b shows the penumbral-spot index used by HS93 digitised from their Figure 8 (dashed red) versus the fraction of penumbral spots we extract from the RGO, Rome, and Debrecen databases after applying an 11-year running mean following HS93. We note that HS93 used the fraction of penumbral spots with reversed ordinate, thus in the following an increase in the penumbral index means a decrease in the fraction of penumbral spots.

We are able to replicate the HS93 penumbral-spot fraction very accurately by simply stitching the RGO data with those from Rome after 1976. However, we note that this approach does not take into account the differences in the two databases, which might be considering completely different regions as penumbral spots and thus they might not be

comparable at all. Furthermore, since we have in our possession more recent data from Rome observatory until 2000 we can also unambiguously conclude that the increasing trend in the penumbral-spot index as used by HS93 since 1980 was yet another artefact of their processing. The decreasing trend of this index continues to 2018 with the Debrecen data. Furthermore, we stress that this index might also be affected by the potential inconsistencies in early RGO group records, as we discussed in Section 2.4, or that these penumbral spots might be at least partly responsible for the reported discrepancies in the early RGO data.

For the following discussion we will use the series we produced by combining RGO and Rome data following HS93, extended to 2000 and then stitched to Debrecen data until 2018. We note that we do not simply stitch the Debrecen data to the other archives because it would introduce a sharp decrease in this index after 2000. In an attempt to reduce the bias in our results due to the archive inconsistencies, we produce two different versions of the penumbral-spot fraction index, where the Debrecen penumbral fractions were divided by three and seven (shown in orange and yellow in Figure 6b, respectively) and stitch these scaled series to the data from the other archives. Both series are shown in Figure 6b. Dividing Debrecen penumbral-spot fractions by three results in a roughly steady decrease after 2000, which is less abrupt than what the original unscaled Debrecen data would give, and reduces to the mean level of penumbral spots at the beginning of the RGO series. Dividing Debrecen penumbral-spot fractions by seven results in an increase to the same level of 1980 and a much slower decrease until the end of the records. Unless otherwise stated, in the following we will use the series where the Debrecen data were divided by three.

3. Combining All Indices to Reconstruct the TSI

In this section, we replicate the methodology of HS93 to reconstruct TSI with the five indices we introduced in the previous section.

As Hoyt and Schatten (1997) mention: "This solar-irradiance model has only two parameters: (1) the amplitude of the solar-cycle variations and (2) the amplitude of the Gleissberg cycle variations." Thus, we can describe this model as having two components, the first one being a solar-cycle component provided from the annual sunspot-number series and the second one being the average of the five indices discussed in the previous section. Each of those components has one free parameter, being the magnitude of their variations.

The scaling of the sunspot number for the first component was determined by simply considering that over $1978 - 1992$ ISNv1 changed by ≈ 150, while Nimbus-7 (Hoyt et al., 1992) TSI measurements changed by ≈ 1.5 W m^{-2}. This led them to the approximate relationship

$$\Delta \mathrm{TSI} = 0.01 \, \mathrm{ISNv1}. \tag{4}$$

Comparing ISNv2 and PMOD TSI composite we find a very similar scaling of

$$\Delta \mathrm{TSI} = 0.0067 \, \mathrm{ISNv2}, \tag{5}$$

which equals 0.01 when brought to the scale of ISNv1 (divided by 0.6) and it is consistent with other more recent studies (Dewitte, Cornelis, and Meftah, 2022; Xu, Lei, and Li, 2021). We show the sunspot-number component in green in Figure 7b.

The second component mentioned by HS93 is derived as the average of the five indices we discussed in Section 2 after linearly scaling them to the TSI. However, there is some ambiguity in the way HS93 scaled these proxies to convert them to TSI values, which we try

to resolve first by using the original HS93 indices and searching for the optimum parameters that allow us to reproduce the final HS93 TSI series.

Then, we use two different approaches of scaling our updated activity indices to reconstruct the TSI:

i) Impose an array of fixed magnitudes of variations for all indices and search for the one that reproduces direct TSI measurements best;
ii) Regress the indices to measured TSI values.

3.1. Reconstructing TSI with Original Indices and Methodology by HS93

Figure 7 shows together all five indices used by HS93 as we digitised them from their Figure 8, that is after they linearly scaled them to the TSI. The first thing that becomes clear is that despite what is stated by HS93, these five series exhibit a considerable disagreement with each other. The differences of the series reach about 3 W m^{-2}, most noticeably after the 1970s, which is greater than the measured solar-cycle variations of TSI (e.g. Fröhlich, 2013; Chatzistergos, Krivova, and Yeo, 2023). The series also disagree on the timings of high activity. For instance, the cycle-decay rate peaks around 1820, at a time when cycle lengths exhibit a deep minimum. Similarly, the peak in the mid-twentieth century occurs at a different time for each index. More strikingly, the highest TSI among all scaled proxies is reached by the smoothed sunspot-number series over the 1990s, which, however, as we discussed in Section 2.1 is entirely due to an artefact of the processing of HS93. Furthermore, the lowest value is reached by the differential rotation index over 1890s, which is at the beginning of the series and thus introduces a discontinuity.

As we already mentioned, these indices were linearly scaled to TSI values, but the exact way the parameters were determined is unclear. Hoyt and Schatten (1993) mention: "All the solar indices which we are proposing as solar irradiance proxies rise from a minimum around 1880 to a maximum in the 1930s. These extremes represent the peak-to-peak irradiance variation for the last century which can have only one value. [...] If the Dalton minimum and the Maunder minimum both had cycle lengths of ≈14 years and therefore similar levels of irradiance, a peak-to-peak variation over the last century of 0.14% to 0.35% is found." In contrast to that, Hoyt and Schatten (1997) mention: "The second parameter is chosen so that the Maunder Minimum will be about 0.25% less bright than the modern Sun, as suggested by Lean and her colleagues (in 1992) [Lean, Skumanich, and White (1992)], based on stellar variations and the brightness of solar faculae and active network."

Based on the above excerpts we consider that HS93 imposed a fixed magnitude of variations between 1880 and 1930 around a mean level of TSI. HS93 further state "For 1979 – 1992 the irradiances are scaled to the mean of the Nimbus-7 measurements.", which we interpret to be the mean level of TSI HS93 used, which we find to be equal to 1372.1 W m^{-2}. Figure 7 shows also the Nimbus-7 TSI measurements along with the five proxies by HS93. We note the striking disagreement between the Nimbus-7 TSI measurements and the various indices used by HS93, in particular the direct measurements show the exact opposite behaviour to that of the various indices. Furthermore, the mean value of Nimbus-7 TSI is higher than most indices.

However, our Figure 8 illustrates clearly that the scaled indices HS93 used do not exhibit the same range of TSI variations between 1880 and the 1930s. The peak of all indices is at almost the same level between 1910 and 1950, however, the minimum values differ and we were unable to find a period that would match the range of TSI variations in all indices. Table 2 lists the magnitude of variations in each index (defined as maximum value minus the minimum one) over three different periods. Table 2 and our Figure 8 suggest that the

Table 2   Range of TSI values (max–min) in W m^{-2} of the five proxy series used by HS93 over three time intervals. The values in parentheses give the percentage of variations relative to a reference level of 1372.1 W m^{-2} (see Section 3.1).

Index	1700 – 1992	1880 – 1930	1880 – 1950
Sunspot number	4.68 (0.34)	1.43 (0.10)	3.10 (0.23)
Cycle length	4.89 (0.36)	2.05 (0.15)	2.64 (0.19)
Cycle-decay rate	4.55 (0.33)	3.31 (0.24)	3.31 (0.24)
Equatorial rotation	4.51 (0.33)	4.51 (0.33)	4.51 (0.33)
Penumbral spots	3.30 (0.24)	3.07 (0.22)	3.30 (0.24)

indices were most likely scaled arbitrarily. However, we find that we can replicate reasonably well the HS93 TSI series by applying a 0.25% magnitude of variations between 1880 and 1950 around a mean level of TSI of 1372.1 W m^{-2}. Figure 7b compares our replication of HS93 TSI series to their final TSI series. We achieve a correlation coefficient of 0.98 and RMS differences of 0.22 W m^{-2} between the series we recover after digitising the proxies from HS93 and their actual TSI reconstruction. Such small differences are unsurprising considering the uncertainties of digitising the indices from poor quality images.

We note that Hoyt and Schatten (1997) justify the estimate of magnitude of TSI variations based on the study by Lean, Skumanich, and White (1992), which was itself based on stellar-activity data by Baliunas and Jastrow (1990). These estimates were later shown to be incorrect (e.g. Hall and Lockwood, 2004; Hall et al., 2009; Wright, 2004) Notwithstanding the ambiguity of how HS93 determined the magnitude of TSI variations, we stress that this was imposed on this reconstruction and was not a result from it.

In our Figure 8 we compare the HS93 reconstructions with four cases of the magnitude of variations to the SATIRE-T (Spectral And Total Irradiance REconstruction, where "T" stands for telescope era; Wu et al., 2018) reconstruction. In particular, we use scalings of 0.25% (the one used by HS93), 0.15%, and 0.05%, and 0% between 1880 and 1950. By imposing a fixed magnitude of 0.25% variations for each index over the period 1880 – 1950 seems appropriate to reasonably replicate the HS93 TSI series. However, the smallest contribution of the five proxy series agrees better with SATIRE-T reconstruction.

In our Figure 8 we also show the reconstruction with a magnitude of variations of 0.25% for which we have removed the temporal lag HS93 introduced to the sunspot-number series and the cycle-decay rates. In this way we also remove the predicted part of the smoothed sunspot-number series HS93 seem to have included, although we stress that this does not remove completely this artefact since the predicted part has influenced the previous six years due to the smoothing process. Strikingly, we note that the peak over 1960 is only marginally lower than the peak in 1950, compared to the sharp decrease the original HS93 series exhibits. This is a critical change, because it shows that even this model, when correcting for some of the processing artefacts, suggests Cycle 19 exhibits a very high level of activity.

3.2. Reconstructing TSI with Updated Indices and Methodology by HS93

In the following, we replicate the HS93 modelling as we defined it in the previous section, but this time using the updated solar-activity indices we presented in Section 2. Figure 9 shows the updated five indices after scaling them to TSI values by imposing a 0.1% magnitude of variations over 1880 – 1950. We note that in contrast to the version of the indices used by HS93, all of the updated indices show a declining trend since at least 1980 (only
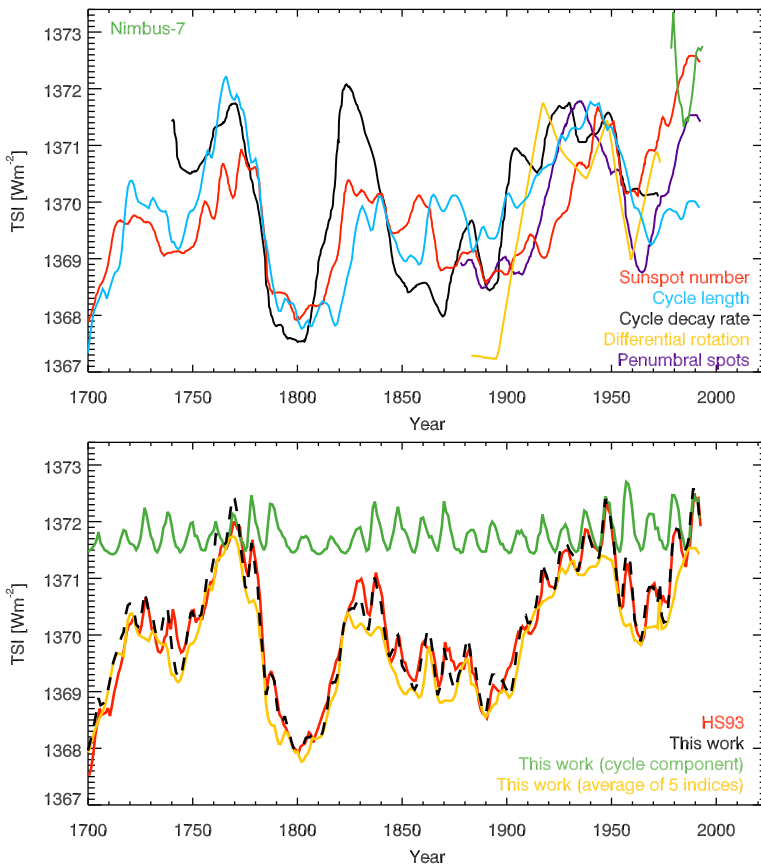
Figure 7 *Top:* The five activity indices used by HS93 to reconstruct the TSI as were presented by them and digitised from their Figure 8. Also shown are the direct TSI measurements by Nimbus-7 (green). *Bottom:* Reconstructed TSI by HS93 (red). Also shown is the average of the five indices shown in the top panel (yellow), the solar-cycle component from the sunspot-number series (green), as well as the combination of the five indices with the solar-cycle component (dashed black). All series are shown as annual means.

the equatorial rotation rate increases again over the last few years), while they still show considerable disagreement over their entire period.

We replicate the methodology of HS93 by scaling all indices separately with a specific magnitude of variations along with the addition of the solar-cycle component from scaling ISNv2 with Equation 5. However, we use a mean TSI level of 1361 W m^{-2} (Kopp and Lean, 2011) derived from more recent and more accurate TSI measurements instead of the one used by HS93. In Figure 10 we show four different versions of our reconstruction where we change the magnitude of variations, in particular 0.25% (the one used by HS93), 0.15%, 0.05%, and 0% over 1880 – 1950. We note that in this process we have to restrict all indices until 2011 due to the limitation imposed by the cycle-length series that applies a 23-year smoothing to the data and requires knowledge of the next solar cycle. This is one drawback of the HS93 modelling, which renders the last 12 years not useful and thus cannot provide a current irradiance reconstruction. We note that HS93 did not exclude the last 12 years of
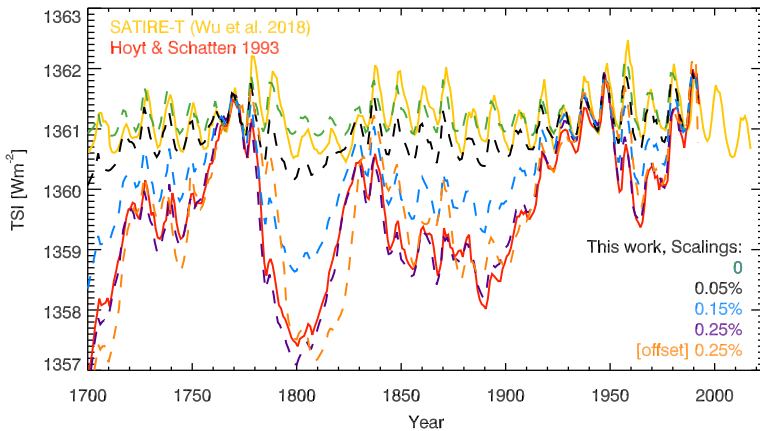
Figure 8 TSI reconstructions with the indices presented by HS93 (dashed series). Shown are four different reconstructions by changing the magnitude of variations over 1880–1950 relative to a reference level of 1361 W m^{-2} to be 0% (dashed green), 0.05% (dashed black), 0.15% (dashed blue), and 0.25% (dashed purple). For the case of the 0.25% scaling we also show the reconstruction for which we correct for the temporal offset of one cycle applied by HS93 to the sunspot number and cycle decay-rate series (orange). Also shown are the SATIRE-T (Wu et al., 2018, yellow) and original HS93 (red) TSI reconstructions. All series were offset to match the value of SATIRE-T over 1986.

the indices, while they seem to have used predicted values for the next solar cycle, and thus they introduced inconsistencies in their produced series as we already discussed.

A striking difference between our update of the HS93 series and the original version is the ranking of solar cycles over the twentieth century. Whereas the original version by HS93 shows a sharp decrease in 1960, our reconstruction with a scaling of 0.25% exhibits only a slight decrease in 1960 compared to the previous activity maximum. Decreasing the scaling of magnitude of variations leads to an increase in the TSI level over 1960, in accordance with most other TSI reconstructions (e.g. Wu et al., 2018; Dasi-Espuig et al., 2016; Lean, 2018; Dewitte, Cornelis, and Meftah, 2022).

Table 3 provides the RMS differences and linear correlation coefficients between our reconstructions and the ACRIM, PMOD, ROB, and Montillet et al. (2022) TSI composite series as well as the modelled TSI series by SATIRE-T (Wu et al., 2018). Comparing to composites of direct TSI measurements and other TSI models we note that the higher the magnitude of variations introduced in the HS93 model the higher the disagreement with the direct measurements is. In particular, the linear correlation between our reconstruction and the different TSI composite series decreases with increasing magnitude of imposed variations, while the RMS differences are lower for the scaling of 0.05%. Scalings greater than 0.07–0.09% result in RMS differences between our reconstructions and TSI composites that become greater than the case of 0% scaling.

The top panel in Figure 10 also compares our reconstructions with the HS93 model and different scalings to the range of uncertainty of direct TSI measurements as defined by Dudok de Wit et al. (2017). The figure clearly highlights the inconsistency of reconstructions with the HS93 model using magnitudes of variations greater than 0.05% to direct measurements of TSI. Overall, the low magnitude of variations suggested by the updated HS93 model with a scaling of 0.05% is in agreement with that reported by the Intergovernmental Panel on Climate Change (IPCC; Matthes et al., 2017; IPCC, 2021; Funke et al., 2023).
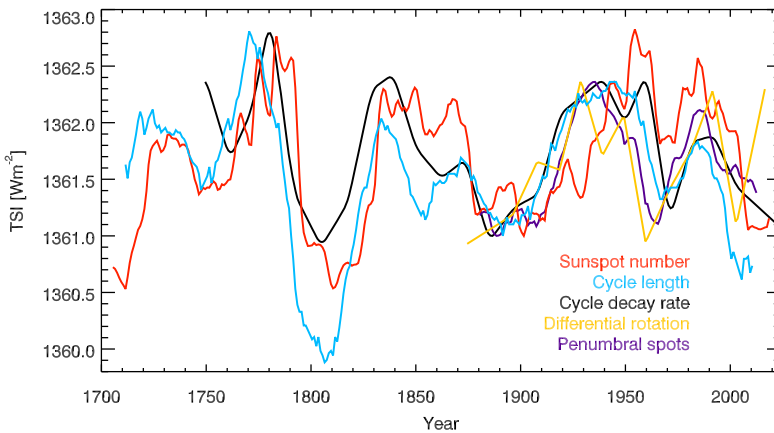
Figure 9 Our updated versions of the five activity indices that were used by HS93 to reconstruct TSI (see Section 2). The series are shown after having scaled them to TSI units by imposing a 0.1% magnitude of variations over the period 1880 – 1950 relative to a reference level of 1361 W m^{-2}.

In Figure 10 we also show the reconstructions with the HS93 model when using the penumbral-spot index with Debrecen data with the two different scalings we introduced in Section 2.5. We find that both scalings return qualitatively the same results, with markedly increasing disagreement between direct TSI measurements and modelled TSI with the HS93 approach.

Finally, we stress that the disagreement between our reconstruction and measured TSI is particularly evident for the ACRIM TSI composite, for which we also report the worse agreement to our reconstructed series. This is in agreement with models reconstructing irradiance in general disfavouring the ACRIM TSI composite (Chatzistergos, Krivova, and Yeo, 2023; Chatzistergos, Krivova, and Ermolli, 2024). We find that no scaling of the proxy indices used by HS93 can lead to a reconstruction that could lend support to the increasing trend in ACRIM between the 1986 and 1996 activity minima, the so-called ACRIM-gap. In particular, we find the exact opposite, that is that the greater the magnitude of imposed variations the higher the decrease between the 1986 and 1996 minima is. As a consequence, the extension of HS93 with the ACRIM TSI composite as was done by Scafetta (2013, 2023) and Scafetta et al. (2019) is utterly inconsistent with the reconstruction with the updated indices. This demonstrates that the high secular trend suggested by the Scafetta (2023) series is an artefact of inappropriate stitching of different data together.

3.3. Reconstructing TSI with Updated Indices and Regression

In this section, we use the activity indices suggested by HS93 to reconstruct TSI by regressing them to direct measurements of TSI. We note that when HS93 released their model, the overlap to direct measurements was not sufficient to take this approach, but now we have data for 30 more years that allows this. We use the Montillet et al. (2022), PMOD, ROB, and ACRIM TSI composite series for the regression after applying an 11-year running mean so as to match the smoothing of the five indices. We regress each index separately and as before we average all of them together and add the solar-cycle component based on Equation 5.

Figure 11a shows the five indices after regressing them to the Montillet et al. (2022) TSI composite series. The amplitude of variations is considerably reduced for all indices, being
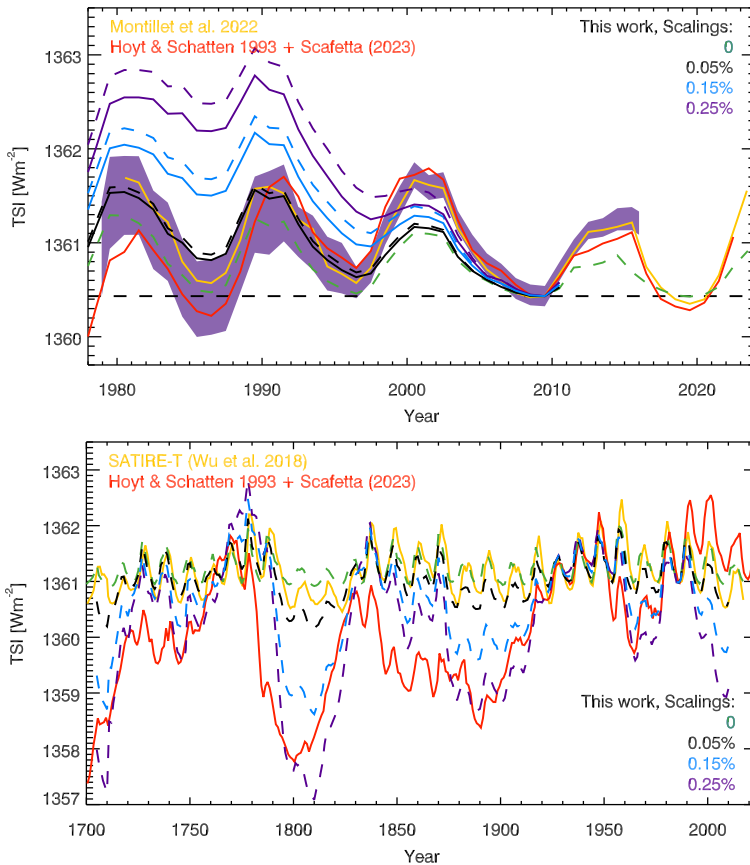
Figure 10 TSI reconstructions with the model of HS93 and using updated data for different scalings of magnitude of variations (solid, only in the upper panel, and dashed lines for the case that Debrecen penumbral-spot fraction was divided by 7 and 3, respectively). Shown are four different reconstructions by changing the magnitude of variations over 1880–1950 relative to a reference level of 1361 W m^{-2} to be 0% (green), 0.05% (black), 0.15% (blue) and 0.25% (purple). Also shown is the Scafetta (2023) series (red) that stitches the HS93 TSI series with the ACRIM TSI composite series as well as SORCE/TIM and TSIS/TIM. The upper panel shows the series over the period of direct measurements offset to match their values during the 2008 activity minimum to that of the Montillet et al. (2022) TSI composite series. We also show the Montillet et al. (2022) TSI composite (yellow) and the 1-σ uncertainty level from the Dudok de Wit et al. (2017) TSI composite (purple shaded surface). The lower panel shows the complete reconstructions back to 1700 along with the SATIRE-T (Wu et al., 2018, yellow) TSI reconstruction offset to match their values during the 1986 activity minimum to that of the SATIRE-T series.

<1 W m^{-2} compared to ≈ 5 W m^{-2} used by HS93. We note, however, that the regression inverts some indices, thus speaking against the applicability of these indices for reconstructing TSI, though the overlapping period might still be insufficient to properly regress the indices to TSI measurements. In particular, this is the case for the equatorial rotation index, which is inverted when considering all composite series used here. Surprisingly, when using ACRIM as the reference the regression inverts all indices and thus returns unrealistic results. This further demonstrates the incompatibility of the HS93 model with the ACRIM TSI composite and thus provides further support against stitching the HS93 series to the ACRIM TSI composite.
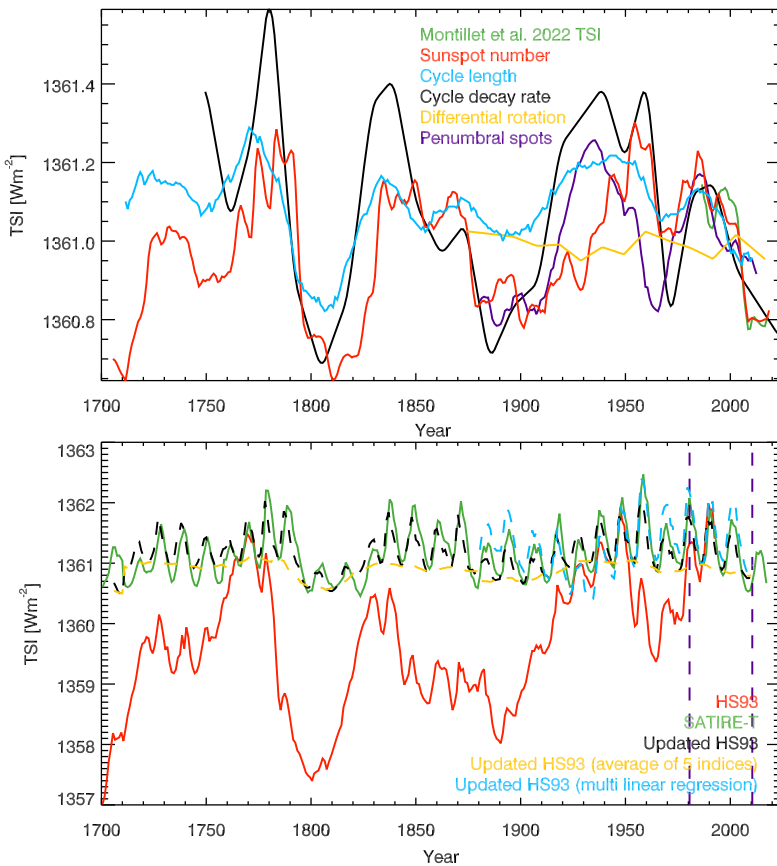
Figure 11 *Top:* Updates of the five activity indices used by HS93 to reconstruct TSI (see Section 2) scaled to TSI units by regression to the Montillet et al. (2022) TSI composite. Also shown is the 11-year smoothed TSI composite series by Montillet et al. (2022, green). *Bottom:* Comparison between the reconstructed TSI by HS93 (red) and the one we obtain by averaging the various activity indices regressed to the Montillet et al. (2022) TSI composite (dashed yellow). The complete reconstruction by averaging the five indices and adding the activity component based on annual sunspot-number series is shown in dashed black. The dashed ciel line shows our reconstruction by performing a multi-linear regression instead of regressing each index separately. Also shown is the SATIRE-T reconstruction by Wu et al. (2018, green). The vertical dashed lines mark the period over which the regression was performed.

The complete TSI reconstruction by averaging the five indices is shown in Figure 11b compared to the original HS93 and SATIRE-T TSI reconstructions, while Table 3 gives the RMS and correlation coefficients between the reconstructed series and each reference TSI series we used. We find that regressing each index to measured TSI returns rather low variations, which is in contrast to the original HS93 reconstruction. This reconstruction with the HS93 model is also consistent with that used by IPCC (Matthes et al., 2017; IPCC, 2021; Funke et al., 2023). In particular, we find the updated HS93 model to exhibit a TSI difference between the 1700s and 1986 of 0.5 W m^{-2} (0.44 W m^{-2} between the 1800s and 1986), which is significantly lower than the 4 W m^{-2} suggested by the original HS93 series.

To render this reconstruction comparable to the one by HS93, we estimated the scaling of the magnitude of the five indices that would result in a TSI series that matches best the
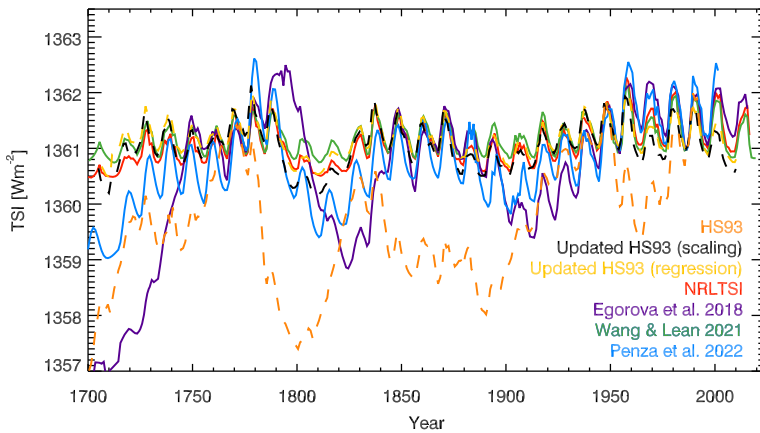
Figure 12 Comparison of our updated TSI reconstruction with the HS93 model and other series from the literature. Shown are annual values offset so that all series match the value of the SATIRE-T reconstruction over 1986.

one produced by regressing the indices to the Montillet et al. (2022) TSI composite. We find a scaling of 0.05% that minimises the RMS differences and maximises the correlation coefficient. This reconstruction is in agreement with the one we reported in Section 3.2, both of them favouring a rather low magnitude of TSI variations since 1700 that are about 0.05% or less. Thus, this approach also disfavours the original HS93 reconstruction as well as its extension by stitching it to ACRIM TSI composite series (Scafetta, 2013, 2023; Scafetta et al., 2019).

We note that we also used a multi-linear regression with all indices together instead of regressing them individually. In this case, however, the reconstruction is limited to the period covered by all indices. The case for using the Montillet et al. (2022) TSI composite as the reference is also shown in ciel in Figure 11b. Unsurprisingly, a multi-linear regression with six indices reproduces the measured TSI data very well for all reference series used, while overall this reconstruction is in agreement with our previous reconstructions from this section and from Section 3.2. However, we find the same issues of inverting the differential rotation index, while for ACRIM it inverts all indices and thus returns inconsistent and unrealistic results for earlier periods.

In Figure 12 we compare our TSI reconstruction by regressing the five activity indices to Montillet et al. (2022) TSI composite series (yellow), as well as our TSI reconstruction from Section 3.2 (black) to other recent TSI reconstructions. Our updated HS93 reconstruction is inconsistent with both the Egorova et al. (2018) and Penza et al. (2022) ones, which suggest a greater magnitude of TSI variations over the last three centuries than ours. The differences between our HS93 reconstruction and Egorova et al. (2018) and Penza et al. (2022) reach 3 W m^{-2} and 1 W m^{-2}, respectively. Although the Egorova et al. (2018) and the original HS93 TSI reconstructions suggest almost the same magnitude of variations, they exhibit significant differences, in particular around 1800 and the second half of the nineteenth and twentieth centuries. Overall, we find our reconstruction with the HS93 model lie closer to the SATIRE-T (Wu et al., 2018), NRLTSI (Lean, 2018) and Wang and Lean (2021) ones.

Table 3 Comparison between published TSI series and our reconstructions of TSI with the HS93 model using our updated indices (see Section 2). Listed are RMS differences in W m^{-2} and linear correlation coefficients in parentheses. The reconstructions with HS93 listed are with a scaling of magnitude of variations of 0%, 0.02%, 0.05%, 0.15% and 0.25% over the period 1880–1950 relative to a reference level of 1361 W m^{-2}, as well as by regressing the indices to published TSI series.

	0%	0.02%	0.05%	0.15%	0.25%	Regression
Montillet et al. (2022)	0.31 (0.96)	0.25 (0.95)	0.21 (0.88)	0.58 (0.65)	1.08 (0.53)	0.23 (0.93)
ACRIM	0.45 (0.84)	0.43 (0.78)	0.42 (0.67)	0.71 (0.40)	1.17 (0.27)	0.51 (0.86)
PMOD	0.29 (0.94)	0.24 (0.91)	0.23 (0.83)	0.63 (0.58)	1.14 (0.46)	0.25 (0.92)
ROB	0.28 (0.97)	0.23 (0.95)	0.23 (0.86)	0.41 (0.55)	0.70 (0.39)	0.21 (0.89)
SATIRE-T	0.37 (0.91)	0.29 (0.91)	0.25 (0.85)	0.66 (0.68)	1.23 (0.61)	0.26 (0.88)

4. Comparison to Earth's Temperatures

Here, we compare the reconstructed TSI with the HS93 model to Earth's temperature measurements. In Figure 13 we show the original HS93 series as well as our updated series after linearly scaling it to Earth's temperature data by HadCRUT5 (Hadley Centre/ Climatic Research Unit Temperature; Osborn et al., 2021, covering the period 1850–2023).[8] We also show the Neukom et al. (2019, covering the period 1–2000) series. The correlation coefficients between the HS93 TSI series and Earth's temperature are given in Table 4. In Table 4 we also show the results for the GISTEMP4 (NASA Goddard Institute for Space Studies Surface Temperature Analysis; Lenssen et al., 2019, covering the period 1880–2023)[9] and Berkeley Earth (Rohde and Hausfather, 2020, covering the period 1850–2023)[10] temperature series. For comparison purposes, Table 4 also lists the correlation coefficient between Earth's temperature and the SATIRE-T (Wu et al., 2018) TSI reconstruction.

We find the original HS93 TSI series exhibits a rather high correlation coefficient of 0.55–0.70 for global temperatures and 0.66–0.73 for northern-hemisphere ones. However, the correlation drops significantly for our updated TSI reconstruction with the HS93 model, being 0.13–0.23 and 0.15–0.18 for global and northern-hemisphere temperatures, respectively. The correlation coefficients are a little higher if we compare our reconstruction to temperatures only over the period 1700–1992, which was the period covered by the original HS93 reconstruction. However, they are still lower than those reported by HS93, being 0.26–0.44 and 0.44–0.51 for the global and northern-hemisphere temperatures, respectively. We also find a generally rather low correlation between SATIRE-T TSI and the various temperature series being between −0.08 and 0.27.

Surprisingly, correcting the original HS93 series for the arbitrary temporal lags in the smoothed sunspot-number series and cycle decay-rate index returns slightly better agreement to the various temperature series. However, we stress that in this process we were unable to remove all artefacts of the original HS93 indices. Furthermore, artefacts in our digitisation of the HS93 indices might be contributing to this too.

Overall, we report a rather low correlation between our version of the HS93 model as well as SATIRE-T TSI and Earth's temperatures. We note that the above simple comparison was not aimed at quantifying the solar impact on temperature variations on Earth (see

---

[8] Available at https://crudata.uea.ac.uk/cru/data/temperature/.

[9] Available at https://data.giss.nasa.gov/gistemp/.

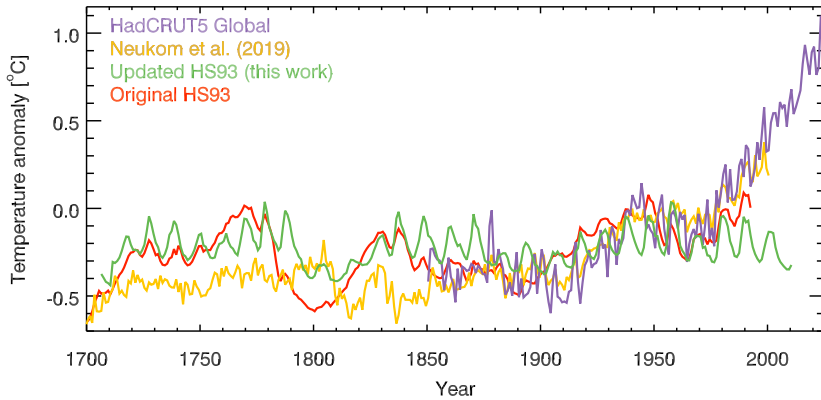[10] Available at https://berkeleyearth.org/data/.

Figure 13 Comparison between Earth-temperature measurements and reconstructed TSI with the HS93 model. Shown are the HadCRUT5 (violet) and Neukom et al. (2019, yellow; offset by 0.25 °C to roughly match the level of HadCRUT5 series) global temperature series along with the HS93 TSI series as originally published (red) and our update of the model as presented in Section 3.3. The TSI series are shown after linearly scaling them to the HadCRUT5 global temperature series. Shown are annual mean values.

Table 4 Correlation coefficients between Earth's temperature measurements and TSI reconstructions with the HS93 model as replicated by us here as well as the original version by HS93 and SATIRE-T.

| | HS93 (Ours) | HS93 (Ours) | HS93 | HS93 (no lags) | SATIRE-T | SATIRE-T |
	$1700-2010$	$1700-1992$	$1700-1992$	$1700-1992$	$1643-2017$	$1700-2010$
HadCRUT5 global	0.16	0.43	0.70	0.71	-0.05	0.02
HadCRUT5 north	0.15	0.44	0.73	0.75	-0.08	-0.01
GISTEMP4 global	0.14	0.44	0.56	0.59	-0.02	0.07
GISTEMP4 north	0.18	0.51	0.66	0.71	-0.03	0.05
Berkeley Earth global	0.13	0.38	0.67	0.68	-0.07	-0.00
Neukom et al. (2019)	0.23	0.26	0.55	0.56	0.27	0.20

e.g. Richardson and Benestad, 2022), but merely to allow us to discuss to what degree the high agreement between the original HS93 TSI series and Earth's temperatures was due to artefacts of their processing.

5. Summary and Conclusions

In this work, we replicated the purely empirical modelling approach by Hoyt and Schatten (1993) by using updated data that extend to the present. This is important in order to assess the quality of the modelling approach, something that was not possible at the time of publication of Hoyt and Schatten (1993) due to the then very short period of direct TSI measurements. First, we highlight that the selection of indices used by Hoyt and Schatten (1993) is rather arbitrary, and some are potentially unsuitable for reconstructing irradiance variations, for instance "penumbral spots" or equatorial rotation. The various indices exhibit significant disagreement with each other, while they also cover different periods, rendering their combination not meaningful. We also note here that all indices used by HS93 are related to sunspots, while they did not consider any facular index (Chatzistergos et al., 2020b;

Chatzistergos, Krivova, and Ermolli, 2022; Chatzistergos et al., 2022), which is another major contributor in irradiance variations. A limiting factor for the HS93 model is that it produces only annual values, while, due to the smoothings applied, it cannot provide consistent results for the first and last 12 years of the used indices. Thus, at any given time this model cannot be used to study the current solar cycle in a consistent way.

We replicated the indices used by HS93 to a rather reasonable degree. However, we find almost perfect agreement only for two out of five indices (smoothed sunspot-number series and penumbral-spot fraction). We discuss sources of uncertainties that contributed to the disagreements of the other indices. These have to do mostly with the vague description of HS93 methodology with potentially hidden steps or artefacts in the processing, as well as potential changes in the data that were used to produce the indices. However, we stress that even for these indices we produce consistently and clearly defined series, while we are still able to qualitatively replicate the indices by HS93 reasonably well to be in position to discuss this TSI modelling approach.

In the process of extracting and reproducing these five indices we revealed various artefacts in the way Hoyt and Schatten (1993) produced them. The most striking one being the arbitrary introduction of an 11-year offset back in time to the 11-year smoothed sunspot-number series, which shifted the peak over the twentieth century by 11 years. This temporal lag is unsupported by modern observations, while we also stress that HS93 introduced it only on the smoothed sunspot-number series and possibly also the cycle-decay rate. This means HS93's analysis treated this lag inconsistently considering that all indices they used were derived from sunspots observed at the surface of the Sun, and thus if such a lag was indeed needed it would affect all of their indices. Furthermore, this artefact was also the reason for an artificial increasing trend of the sunspot-number series over the last decade of the data, because HS93 had to estimate the values of the next cycle so as to allow extending this index to 1992 after having shifted it back in time by 11 years. This is effectively the same type of artefact that was introduced by Friis-Christensen and Lassen (1991) in their determination of their cycle-length series (Chatzistergos, 2023). We also reported an inappropriate combination of penumbral-spot data from different sources, such that it also introduced an artificial increase at the end of the series.

Our updates of the various indices with more recent data revealed that the increasing TSI trend suggested by Hoyt and Schatten (1993) after 1960 was purely an artefact of their processing. More importantly, our analysis allows us to better define one of the free parameters of this model, the magnitude of TSI variations, by comparing the reconstruction to direct measurements of TSI. This was not possible at the time of publication of the original HS93 model due to the short period of direct TSI measurements, which is why HS93 set this parameter based on estimates from stellar-activity studies, which were later shown to be incorrect (e.g. Hall and Lockwood, 2004; Hall et al., 2009; Wright, 2004). We find that the best agreement of the updated HS93 model to direct TSI measurements and other published models is achieved when we minimise the average of the five indices with a magnitude of variations of about 0.05% or less, that is one fifth or lower than the magnitude that was imposed by HS93. We also note that we find a poor agreement between our reconstruction with the HS93 model and ACRIM TSI composite series. This renders the extensions of the Hoyt and Schatten (1993) TSI series with the ACRIM TSI composite, as was done by Scafetta (2013, 2023) and Scafetta et al. (2019), entirely wrong. This is particularly important because it shows that such extensions of the Hoyt and Schatten (1993) TSI model with measured TSI data introduce an entirely artificial secular trend in TSI variations that is not supported even by this model.

We note that one could have also reached the conclusion that the original HS93 TSI series suggests implausible TSI variations also with a simple qualitative argument. That is,

by considering that the 11-year smoothed sunspot-number series exhibits similar levels over Cycle 24 and the beginning of the 1900s. Considering that all five proxies used by HS93 are supposed to be in a good agreement they should all approximately mirror the behaviour of the smoothed sunspot-number series, at least in terms of magnitude of variations. Further considering that the difference between the minimum at the beginning of Solar Cycle 22 and 14 in the original HS93 TSI series is about 2 W m^{-2} one would expect the difference between the minimum of Solar Cycles 22 and 24 to be about 2 W m^{-2} as well. This is in contrast to actual measurements of TSI over that period (e.g. Dudok de Wit et al., 2017; Montillet et al., 2022; Chatzistergos, Krivova, and Yeo, 2023, and references therein) as well as the extension of the original HS93 series with ACRIM by Scafetta (2023). This simple qualitative argument should have sufficed to expect that the extension of HS93 by Scafetta (2023), as well as the high magnitude of the long-term trend in the original HS93 model were rather unrealistic.

Overall, our work highlighted issues with the original HS93 TSI series by identifying artefacts in the processing HS93 applied, while also discussing the issues with the arbitrary choice of activity indices used by this model. In addition, by updating the activity indices the model uses, we demonstrated that the original HS93 TSI series suggests an implausible magnitude of variations, which is incompatible with recent TSI data. We also showed that replicating and updating the HS93 model with recent data results in TSI variations since 1700 that are consistent with those by SATIRE-T and NRLTSI, that is those used by IPCC. In particular, the updated HS93 model suggests a TSI difference between the 1700s and 1986 of 0.5 W m^{-2}, which is significantly lower than the 4 W m^{-2} suggested by the original HS93 series. Finally, we found the updated TSI series with the HS93 model exhibits a rather poor agreement with Earth's temperature (linear correlation coefficients between 0.13 and 0.23 when considering the entire period of TSI reconstruction, 1700 – 2010). This demonstrates that the high agreement that was previously reported is due to artefacts in the processing applied by HS93 and the exaggerated magnitude of variations they imposed. As a consequence, this also renders void arguments about the solar influence on Earth's climate that were drawn based on the original HS93 series (e.g. Connolly et al., 2020, 2021; Scafetta, 2023; Soon et al., 2023; Georgieva and Veretenenko, 2023).

Had these issues been realised earlier, the Hoyt and Schatten (1993) series would have been rather unlikely to have received the attention it did. We also hope that this work highlights the importance of attempting to replicate other studies, to avoid such issues in the future.

Data Availability Data produced in this study can be made available upon request.

Declarations

Competing interests The authors declare no competing interests.

References

Amdur, T., Stine, A.R., Huybers, P.: 2021, Global surface temperature response to 11-yr solar cycle forcing consistent with general circulation model results. *J. Climate* **34**(8), 2893.

Arlt, R., Leussu, R., Giese, N., et al.: 2013, Sunspot positions and sizes for 1825 – 1867 from the observations by Samuel Heinrich Schwabe. *Mon. Not. Roy. Astron. Soc.* **433**, 3165. DOI. ADS.

Baliunas, S., Jastrow, R.: 1990, Evidence for long-term brightness changes of solar-type stars. *Nature* **348**, 520. DOI. ADS.

Baranyi, T.: 2015, Comparison of debrecen and mount Wilson/kodaikanal sunspot group tilt angles and the joy's law. *Mon. Not. Roy. Astron. Soc.* **447**, 1857. DOI. ADS.

Bard, E., Raisbeck, G., Yiou, F., et al.: 2000, Solar irradiance during the last 1200 years based on cosmogenic nuclides. *Tellus, Ser. B Chem. Phys. Meteorol. B* **52**, 985. DOI. ADS.

Bhattacharya, S., Lefevre, L., Chatzistergos, T., Hayakawa, H., Jansen, M.: 2023, Rudolf Wolf to Alfred Wolfer: the Transfer of the Reference Observer. In the International Sunspot Number Series (1876 – 1893). *Solar Phys.*, in press. DOI.

Biswas, A., Karak, B.B., Usoskin, I., et al.: 2023, Long-term modulation of solar cycles. *Space Sci. Rev.* **219**(3), 19. DOI.

Carrasco, V.M.S., Vaquero, J.M., Gallego, M.C.: 2021, A forgotten sunspot record during the Maunder minimum (Jean Charles Gallet, 1677). *Publ. Astron. Soc. Japan* **73**(3), 747. DOI.

Carrasco, V.M.S., Nogales, J.M., Vaquero, J.M., et al.: 2021, A note on the sunspot and prominence records made by Angelo Secchi during the period 1871 – 1875. *J. Space Weather Space Clim.* **11**, 51. DOI.

Chatzistergos, T.: 2023, Is there a link between the length of the solar cycle and Earth's temperature? *Rend. Lincei, Sci. Fis. Nat.* **34**(1), 11. DOI.

Chatzistergos, T., Krivova, N.A., Ermolli, I.: 2022, Full-disc Ca II K observations - a window to past solar magnetism. *Front. Astron. Space Sci.* **9**. DOI.

Chatzistergos, T., Krivova, N., Ermolli, I.: 2024, Understanding the secular variability of solar irradiance: the potential of Ca II K observations. JSWSC.

Chatzistergos, T., Krivova, N.A., Yeo, K.L.: 2023, Long-term changes in solar activity and irradiance. *J. Atmos. Solar-Terr. Phys.* **252**, 106150. DOI.

Chatzistergos, T., Usoskin, I.G., Kovaltsov, G.A., et al.: 2017, New reconstruction of the sunspot group numbers since 1739 using direct calibration and "backbone" methods. *Astron. Astrophys.* **602**, A69. DOI.

Chatzistergos, T., Ermolli, I., Giorgi, F., et al.: 2020a, Modelling solar irradiance from ground-based photometric observations. *J. Space Weather Space Clim.* **10**, 45. DOI.

Chatzistergos, T., Ermolli, I., Krivova, N.A., et al.: 2020b, Analysis of full-disc Ca II K spectroheliograms - III. Plage area composite series covering 1892 – 2019. *Astron. Astrophys.* **639**, A88. DOI.

Chatzistergos, T., Krivova, N.A., Ermolli, I., et al.: 2021, Reconstructing solar irradiance from historical Ca II K observations - I. Method and its validation. *Astron. Astrophys.* **656**, A104. DOI.

Chatzistergos, T., Ermolli, I., Krivova, N.A., et al.: 2022, Scrutinising the relationship between plage areas and sunspot areas and numbers. *Astron. Astrophys.* **667**, A167. DOI.

Clette, F., Lefèvre, L.: 2016, The new sunspot number: assembling all corrections. *Solar Phys.* **291**(9 – 10), 2629. DOI.

Clette, F., Svalgaard, L., Vaquero, J.M., et al.: 2014, Revisiting the sunspot number: a 400-year perspective on the solar cycle. *Space Sci. Rev.* **186**(1 – 4), 35. DOI.

Clette, F., Lefèvre, L., Bechet, S., et al.: 2021, Reconstruction of the sunspot number source database and the 1947 Zurich discontinuity. *Solar Phys.* **296**(9), 137. DOI.

Clette, F., Lefèvre, L., Chatzistergos, T., et al.: 2023, Recalibration of the sunspot-number: status report. *Solar Phys.* **298**(3), 44. DOI.

Cliver, E.W., Ling, A.G.: 2016, The discontinuity circa 1885 in the group sunspot number. *Solar Phys.* **291**(9 – 10), 2763. DOI.

Connolly, R., Connolly, M., Carter, R., et al.: 2020, How much human-caused global warming should we expect with business-as-usual (BaU) climate policies? A semi-empirical assessment. *Energies* 16(3). DOI.

Connolly, R., Soon, W., Connolly, M., et al.: 2021, How much has the Sun influenced Northern Hemisphere temperature trends? An ongoing debate. *Res. Astron. Astrophys.* **21**(6), 131. DOI.

Connolly, R., Soon, W., Connolly, M., et al.: 2023, Challenges in the detection and attribution of Northern Hemisphere surface temperature trends since 1850. *Res. Astron. Astrophys.* **23**(10), 105015. DOI.

Dasi-Espuig, M., Jiang, J., Krivova, N.A., et al.: 2016, Reconstruction of spectral solar irradiance since 1700 from simulated magnetograms. *Astron. Astrophys.* **590**, A63. DOI. ADS.

Delaygue, G., Bard, E.: 2011, An Antarctic view of Beryllium-10 and solar activity for the past millennium. *Clim. Dyn.* **36**, 2201. DOI. ADS.

Dewitte, S., Cornelis, J., Meftah, M.: 2022, Centennial total solar irradiance variation. *Remote Sens.* **14**(5), 1072. DOI.

Dewitte, S., Crommelynck, D., Joukoff, A.: 2004, Total solar irradiance observations from DIARAD/VIRGO. *J. Geophys. Res. Space Phys.* **109**, A02102. DOI. ADS.

Dewitte, S., Nevens, S.: 2016, The total solar irradiance climate data record. *Astrophys. J.* **830**, 25. DOI. ADS.

Dicke, R.H.: 1979, Solar luminosity and the sunspot cycle. *Nature* **280**, 24. DOI. ADS.

Dudok de Wit, T., Kopp, G., Fröhlich, C., et al.: 2017, Methodology to create a new total solar irradiance record: making a composite out of multiple data records. *Geophys. Res. Lett.* **44**(3), 1196. DOI.

Egorova, T., Schmutz, W., Rozanov, E., et al.: 2018, Revised historical solar irradiance forcing. *Astron. Astrophys.* **615**, A85. DOI. ADS.

Ermolli, I., Chatzistergos, T.: 2023, Reconstructing solar irradiance over the period 1996 – 2022. In: *EGU23. Copernicus Meetings.* DOI.

Ermolli, I., Chatzistergos, T., Giorgi, F., et al.: 2023, Solar observations by Angelo Secchi. I. Digitization of original documents and analysis of group numbers over the period of 1853 – 1878. *Astrophys. J. Suppl.* **269**(2), 53. DOI.

Friis-Christensen, E., Lassen, K.: 1991, Length of the solar cycle: an indicator of solar activity closely associated with climate. *Science* **254**, 698. DOI. ADS.

Fröhlich, C.: 2006, Solar irradiance variability since 1978. Revision of the PMOD composite during solar cycle 21. *Space Sci. Rev.* **125**, 53. DOI. ADS.

Fröhlich, C.: 2013, Total solar irradiance: what have we learned from the last three cycles and the recent minimum? *Space Sci. Rev.* **176**, 237. DOI. ADS.

Funke, B., Dudok de Wit, T., Ermolli, I., et al.: 2023, Towards the definition of a solar forcing dataset for CMIP7. *Geosci. Model Dev. Discuss.*, 1. DOI.

Georgieva, K., Veretenenko, S.: 2023, Solar influences on the Earth's atmosphere: solved and unsolved questions. *Front. Astron. Space Sci.* **10**, 1244402. DOI. ADS.

Hall, J.C., Lockwood, G.W.: 2004, The chromospheric activity and variability of cycling and flat activity solar-analog stars. *Astrophys. J.* **614**, 942. DOI. ADS.

Hall, J.C., Henry, G.W., Lockwood, G.W., et al.: 2009, The activity and variability of the sun and sun-like stars. II. Contemporaneous photometry and spectroscopy of bright solar analogs. *Astron. J.* **138**, 312. DOI. ADS.

Hathaway, D.H.: 2015, The solar cycle. *Living Rev. Solar Phys.* **12**(1), 4. DOI.

Hayakawa, H., Iju, T., Kuroyanagi, C., et al.: 2021a, Johann Christoph Müller's sunspot observations in 1719 - 1720: snapshots of the immediate aftermath of the Maunder minimum. *Solar Phys.* **296**(10), 154. DOI.

Hayakawa, H., Iju, T., Uneme, S., et al.: 2021b, Reanalyses of the sunspot observations of Fogelius and Siverus: two 'long-term' observers during the Maunder minimum. *Mon. Not. Roy. Astron. Soc.* **506**(1), 650. DOI.

Herschel, W.: 1801, Observations tending to investigate the nature of the Sun, in order to find the causes or symptoms of its variable emission of light and heat; with remarks on the use that may possibly be drawn from solar observations. *Phil. Trans. Roy. Soc. London* **91**, 265. http://www.jstor.org/stable/107097.

Hoyt, D.V.: 1990, Using the boundary conditions of sunspots as a technique for monitoring solar luminosity variations. In: Schatten, K.H., Arking, A. (eds.) *NASA Conf. Publ., CP-3086.* https://ntrs.nasa.gov/citations/19910003150.

Hoyt, D.V., Schatten, K.H.: 1993, A discussion of plausible solar irradiance variations, 1700 – 1992. *J. Geophys. Res.* **98**, 18. DOI. ADS

Hoyt, D.V., Schatten, K.H.: 1997, *The Role of the Sun in Climate Change*, Oxford University Press, New York.

Hoyt, D.V., Kyle, H.L., Hickey, J.R., et al.: 1992, The Nimbus 7 solar total irradiance: a new algorithm for its derivation. *J. Geophys. Res.* **97**, 51. DOI. ADS.

IPCC: 2021, *Climate Change 2021: The Physical Science Basis. Contribution of Working Group I to the Sixth Assessment Report of the Intergovernmental Panel on Climate Change*, Cambridge University Press, Cambridge. DOI.

Javaraiah, J.: 2011, Long-term variations in the growth and decay rates of sunspot groups. *Solar Phys.* **270**, 463. DOI. ADS.

Javaraiah, J., Bertello, L., Ulrich, R.K.: 2005, Long-term variations in solar differential rotation and sunspot activity. *Solar Phys.* **232**(1), 25. DOI.

Jha, B.K., Priyadarshi, A., Mandal, S., et al.: 2021, Measurements of solar differential rotation using the century long kodaikanal sunspot data. *Solar Phys.* **296**(1), 25. DOI.

Kopp, G.: 2016, Magnitudes and timescales of total solar irradiance variability. *J. Space Weather Space Clim.* **6**, A30. DOI. ADS.

Kopp, G.: 2021, Science highlights and final updates from 17 years of total solar irradiance measurements from the SOlar radiation and climate experiment/total irradiance monitor (SORCE/TIM). *Solar Phys.* **296**, 133. DOI. ADS.

Kopp, G., Lean, J.L.: 2011, A new, lower value of total solar irradiance: evidence and climate significance. *Geophys. Res. Lett.* **38**, L01706. DOI. ADS.

Kren, A.C., Pilewskie, P., Coddington, O.: 2017, Where does Earth's atmosphere get its energy? *J. Space Weather Space Clim.* **7**, A10. DOI. ADS.

Krivova, N.A.: 2018, Solar irradiance variability and Earth's climate. In: *Climate Changes in the Holocene*, CRC Press, Boca Raton, 107. DOI.

Krivova, N.A., Balmaceda, L., Solanki, S.K.: 2007, Reconstruction of solar total irradiance since 1700 from the surface magnetic flux. *Astron. Astrophys.* **467**, 335. DOI. ADS.

Krivova, N.A., Vieira, L.E.A., Solanki, S.K.: 2010, Reconstruction of solar spectral irradiance since the Maunder minimum. *J. Geophys. Res. Space Phys.* **115**, 12112. DOI. ADS.

Krivova, N.A., Solanki, S.K., Fligge, M., et al.: 2003, Reconstruction of solar irradiance variations in cycle 23: is solar surface magnetism the cause? *Astron. Astrophys.* **399**, L1. DOI. ADS.

Lamb, D.A.: 2017, Measurements of solar differential rotation and meridional circulation from tracking of photospheric magnetic features. *Astrophys. J.* **836**(1), 10. DOI.

Lean, J.L.: 2018, Estimating solar irradiance since 850 CE. *Earth Space Sci.* **5**(4), 133. DOI.

Lean, J., Skumanich, A., White, O.: 1992, Estimating the Sun's radiative output during the Maunder minimum. *Geophys. Res. Lett.* **19**, 1591. DOI. ADS.

Lefevre, L., Clette, F.: 2014, Survey and merging of sunspot catalogs. *Solar Phys.* **289**, 545. DOI. ADS.

Lenssen, N.J.L., Schmidt, G.A., Hansen, J.E., et al.: 2019, Improvements in the GISTEMP uncertainty model. *J. Geophys. Res., Atmos.* **124**(12), 6307. DOI.

Lockwood, M., Ball, W.T.: 2020, Placing limits on long-term variations in quiet-Sun irradiance and their contribution to total solar irradiance and solar radiative forcing of climate. *Proc. Roy. Soc., Math. Phys. Eng. Sci.* **476**(2238), 20200077. DOI.

Lockwood, M., Owens, M.J., Barnard, L., et al.: 2016, An assessment of sunspot number data composites over 1845 – 2014. *Astrophys. J.* **824**, 54. DOI. ADS.

Love, J.J.: 2013, On the insignificance of Herschel's sunspot correlation: HERSCHEL'S HYPOTHESIS. *Geophys. Res. Lett.* **40**(16), 4171. DOI.

Marchenko, S.V., Lean, J.L., DeLand, M.T.: 2022, Relationship between total solar irradiance and magnetic flux during solar minima. *Astrophys. J.* **936**(2), 158. DOI.

Matthes, K., Funke, B., Andersson, M.E., et al.: 2017, Solar forcing for CMIP6 (v3.2). *Geosci. Model Dev.* **10**(6), 2247. DOI.

Mishra, D.K., Routh, S., Jha, B.K., et al.: 2024, Differential rotation of the solar chromosphere: a century-long perspective from Kodaikanal solar observatory Ca ii K data. *Astrophys. J.* **961**(1), 40. DOI.

Misios, S., Mitchell, D.M., Gray, L.J., et al.: 2016, Solar signals in CMIP-5 simulations: effects of atmosphere–ocean coupling. *Q. J. Roy. Meteorol. Soc.* **142**(695), 928. DOI.

Montillet, J.P., Finsterle, W., Kermarrec, G., et al.: 2022, Data fusion of total solar irradiance composite time series using 41 years of satellite measurements. *J. Geophys. Res., Atmos.* **127**(13), e2021JD036146. DOI.

Nandy, D.: 2021, Progress in solar cycle predictions: sunspot cycles 24 – 25 in perspective. *Solar Phys.* **296**(3), 54. DOI.

Neukom, R., Barboza, L.A., Erb, M.P., et al.: 2019, Consistent multidecadal variability in global temperature reconstructions and simulations over the common era. *Nat. Geosci.* **12**(8), 643. DOI.

Osborn, T.J., Jones, P.D., Lister, D.H., et al.: 2021, Land surface air temperature variations across the globe updated to 2019: the CRUTEM5 data set. *J. Geophys. Res., Atmos.* **126**(2), e2019JD032352. DOI.

Penza, V., Berrilli, F., Bertello, L., et al.: 2022, Total solar irradiance during the last five centuries. *Astrophys. J.* **937**(2), 84. DOI.

Pesnell, W.D.: 2016, Predictions of solar cycle 24: how are we doing?. *Space Weather* **14**, 10. DOI. ADS.

Petrovay, K.: 2020, Solar cycle prediction. *Living Rev. Solar Phys.* **17**(1), 2. DOI.

Pilewskie, P., Kopp, G., Richard, E., et al.: 2018, TSIS-1 and continuity of the total and spectral solar irradiance climate data record. In: *Proceedings from the 20th EGU General Assembly*, *held 4 – 13 April, 2018 Vienna, Austria*, 5527. ADS.

Richardson, M.T., Benestad, R.E.: 2022, Erroneous use of statistics behind claims of a major solar role in recent warming. *Res. Astron. Astrophys.* **22**(12), 125008. DOI.

Rohde, R.A., Hausfather, Z.: 2020, The Berkeley Earth land/ocean temperature record. *Earth Syst. Sci. Data* **12**, 3469. DOI.

Roša, D., Brajša, R., Vršnak, B., et al.: 1995, The relation between the synodic and sidereal rotation period of the Sun. *Solar Phys.* **159**, 393. DOI. ADS.

Sakurai, K.: 1977, Equatorial solar rotation and its relation to climatic changes. *Nature* **269**, 401. DOI ADS.

Sarychev, A.P., Roshchina, E.M.: 2009, Comparison of three solar activity indices based on sunspot observations. *Solar Syst. Res.* **43**, 151. DOI. ADS.

Scafetta, N.: 2013, Olar and planetary oscillation control on climate change: hind-cast, forecast and a comparison with the Cmip5 Gcms. *Energy Environ.* **24**(3 – 4), 455. DOI.

Scafetta, N.: 2023, Empirical assessment of the role of the Sun in climate change using balanced multi-proxy solar records. *Geosci. Front.* **14**(6), 101650. DOI.

Scafetta, N., Willson, R.C., Lee, J.N., et al.: 2019, Modeling quiet solar luminosity variability from TSI satellite measurements and proxy models during 1980 – 2018. *Remote Sens.* **11**(21), 2569. DOI.

Shapiro, A.I., Schmutz, W., Rozanov, E., et al.: 2011, A new approach to the long-term reconstruction of the solar irradiance leads to large historical solar forcing. *Astron. Astrophys.* **529**, 67. DOI. ADS.

Shapiro, A.I., Solanki, S.K., Krivova, N.A., et al.: 2017, The nature of solar brightness variations. *Nat. Astron.* **1**, 612. DOI. ADS.

Similä, M., Usoskin, I.: 2022, Solar cycles reconstructed over the last millennium: do waldmeier and Gnevysev-Ohl rules work?. *Proc. Int. Astron. Union* **18**(S372), 70. DOI.

Skokić, I., Brajša, R., Roša, D., et al.: 2014, Validity of the relations between the synodic and sidereal rotation velocities of the Sun. *Solar Phys.* **289**, 1471. DOI. ADS.

Solanki, S.K., Krivova, N.A., Haigh, J.D.: 2013, Solar irradiance variability and climate. *Annu. Rev. Astron. Astrophys.* **51**(1), 311. DOI.

Soon, W., Connolly, R., Connolly, M.: 2015, Re-evaluating the role of solar variability on Northern Hemisphere temperature trends since the 19th century. *Earth-Sci. Rev.* **150**, 409. DOI.

Soon, W., Connolly, R., Connolly, M., et al.: 2023, The detection and attribution of Northern Hemisphere land surface warming (1850 – 2018) in terms of human and natural factors: challenges of inadequate data. *Climate* **11**(9), 179. DOI.

Usoskin, I.G., Kovaltsov, G.A., Chatzistergos, T.: 2016, Dependence of the sunspot-group size on the level of solar activity and its influence on the calibration of solar observers. *Solar Phys.* **291**(12), 3793. DOI.

Usoskin, I., Kovaltsov, G., Kiviaho, W.: 2021, Robustness of solar-cycle empirical rules across different series including an updated active-day fraction (ADF) sunspot group series. *Solar Phys.* **296**(1), 13. DOI.

Usoskin, I.G., Kovaltsov, G.A., Lockwood, M., et al.: 2016, A new calibrated sunspot group series since 1749: statistics of active day fractions. *Solar Phys.* **291**(9 – 10), 2685. DOI.

Vaquero, J.M., Svalgaard, L., Carrasco, V.M.S., et al.: 2016, A revised collection of sunspot group numbers. *Solar Phys.* **291**(9 – 10), 3061. DOI.

Vieira, L.E.A., Solanki, S.K., Krivova, N.A., et al.: 2011, Evolution of the solar irradiance during the Holocene. *Astron. Astrophys.* **531**, 6. DOI. ADS.

Waldmeier, M.: 1961, The sunspot-activity in the years 1610 – 1960. Zürich Schulthess and Co AG. ADS.

Wang, Y.M., Lean, J.L.: 2021, A new reconstruction of the sun's magnetic field and total irradiance since 1700. *Astrophys. J.* **920**, 100. DOI. ADS.

Weisshaar, E., Cameron, R.H., Schüssler, M.: 2023, No evidence for synchronization of the solar cycle by a "clock". *Astron. Astrophys.* **671**, A87. DOI.

Willson, R.C.: 1997, Total solar irradiance trend during solar cycles 21 and 22. *Science* **277**, 1963. DOI. ADS.

Willson, R.C., Mordvinov, A.V.: 2003, Composite total solar irradiance time series show a secular 0.04%/decade trend. In: *AGU Fall Meeting Abstracts 31*. ADS.

Wittmann, A.D.: 1996, On the relation between the synodic and sidereal rotation period of the Sun. *Solar Phys.* **168**(1), 211. DOI.

Wright, J.T.: 2004, Do we know of any Maunder minimum stars? *Astron. J.* **128**(3), 1273. DOI.

Wu, C.J., Krivova, N.A., Solanki, S.K., et al.: 2018, Solar total and spectral irradiance reconstruction over the last 9000 years. *Astron. Astrophys.* **620**, A120. DOI.

Xu, H., Lei, B., Li, Z.: 2021, A reconstruction of total solar irradiance based on wavelet analysis. *Earth Space Sci.* **8**(10), e2021EA001819. DOI.

Yeo, K.L., Solanki, S.K., Norris, C.M., et al.: 2017, Solar Irradiance Variability is Caused by the Magnetic Activity on the Solar Surface. *Phys. Rev. Lett.* 119. DOI. ADS.

Yeo, K.L., Krivova, N.A., Solanki, S.K., et al.: 2014, Reconstruction of total and spectral solar irradiance from 1974 to 2013 based on KPVT, SoHO/MDI, and SDO/HMI observations. *Astron. Astrophys.* **570**, A85. DOI. ADS.

Yeo, K.L., Solanki, S.K., Krivova, N.A., et al.: 2020, The dimmest state of the Sun. *Geophys. Res. Lett.* **47**(19), e2020GL090243. DOI.